bioRxiv preprint doi: https://doi.org/10.1101/2023.01.25.525485; this version posted January 25, 2023. The copyright holder for this preprint (which was not certified by peer review) is the author/funder, who has granted bioRxiv a license to display the preprint in perpetuity. It is made available under aCC-BY-ND 4.0 International license.

Long-term respiratory mucosal immune memory to SARS-CoV-2 after infection and vaccination

Elena Mitsi[1,2*], Mariana O. Diniz[3*], Jesús Reiné [1,2], Andrea M. Collins[2], Ryan Robinson[2], Angela Hyder-Wright[2], Madlen Farrar[2], Konstantinos Liatsikos[2], Josh Hamilton[2], Onyia Onyema[2], Britta C. Urban[1,2], Carla Solorzano[1,2], Teresa Lambe[1,5], Simon J. Draper[4], Daniela Weiskopf[6], Alessandro Sette[6,7], Mala K. Maini[3^] and Daniela M. Ferreira[1,2^]

[1] Oxford Vaccine Group, Department of Paediatrics, University of Oxford, Oxford, UK.
[2] Department of Clinical Science, Liverpool School of Tropical Medicine, Liverpool, UK.
[3] Division of Infection and Immunity and Institute of Immunity and Transplantation, UCL, London, UK.
[4]Department of Biochemistry, University of Oxford, Oxford, UK
[5]Chinese Academy of Medical Science (CAMS) Oxford Institute (COI), University of Oxford, Oxford, UK
[6]Center for Infectious Disease and Vaccine Research, La Jolla Institute for Immunology (LJI), La Jolla, USA.
[7]Department of Medicine, Division of Infectious Diseases and Global Public Health, University of California, San Diego, La Jolla, USA.

*Joint first authors
^Joint senior authors.

Corresponding: elena.mitsi@paediatrics.ox.ac.uk, daniela.ferreira@paediatrics.ox.ac.uk

bioRxiv preprint doi: https://doi.org/10.1101/2023.01.25.525485; this version posted January 25, 2023. The copyright holder for this preprint (which was not certified by peer review) is the author/funder, who has granted bioRxiv a license to display the preprint in perpetuity. It is made available under aCC-BY-ND 4.0 International license.

ABSTRACT

Respiratory mucosal immunity induced by vaccination is vital for protection from coronavirus infection in animal models. In humans, SARS-CoV-2 immunity has been studied extensively in blood. However, the capacity of peripheral vaccination to generate sustained humoral and cellular immunity in the lung mucosa, and how this is influenced by prior SARS-CoV-2 infection, is unknown. Bronchoalveolar lavage samples obtained from vaccinated donors with or without prior infection revealed enrichment of spike-specific antibodies, class-switched memory B cells and T cells in the lung mucosa compared to the periphery in the setting of hybrid immunity, whereas in the context of vaccination alone, local anti-viral immunity was limited to antibody responses. Spike-specific T cells persisted in the lung mucosa for up to 5 months post-vaccination and multi-specific T cell responses were detected at least up to 11 months post-infection. Thus, durable lung mucosal immunity against SARS-CoV-2 seen after hybrid exposure cannot be achieved by peripheral vaccination alone, supporting the need for vaccines targeting the airways.

Key words: human lung mucosa, hybrid immunity, SARS-CoV-2 vaccination, airway memory T cells

bioRxiv preprint doi: https://doi.org/10.1101/2023.01.25.525485; this version posted January 25, 2023. The copyright holder for this preprint (which was not certified by peer review) is the author/funder, who has granted bioRxiv a license to display the preprint in perpetuity. It is made available under aCC-BY-ND 4.0 International license.

INTRODUCTION

Respiratory mucosal surfaces are the primary site of interaction between SARS-CoV-2 and the immune system. Mucosal antibodies and tissue-resident memory T (TRM) and B cells provide frontline early responses, contributing to protection against the establishment of viral infection following previous viral exposure or vaccination [1, 2 3]. Animal studies of influenza virus infection have shown that development of antigen-specific resident memory B cells in the lung produces local IgG and IgA with enhanced cross-recognition of variants[4] and correlates with protection against reinfection in mice[5, 6]. Additionally, studies of respiratory viral infections in animals and human controlled challenge have highlighted the essential role of local tissue-memory T cells in promoting immunity against influenza and respiratory syncytial virus (RSV) mediated, at least in part, by rapid IFN-γ production[7, 8, 9, 10, 11, 12]. Interestingly, in a murine model of SARS-1 and MERS coronavirus infection, protection was attributed to the induction of $CD4^+$ T cells in the airway [13].

The difficulty accessing human mucosal sites, particularly the lower airways, and the low recovery of fluid and cell yield, have hindered the study of local immunity to respiratory pathogens. Most of the human studies have assessed antibody and T cell responses to SARS-CoV-2 in blood, which is often not reflective of the responses in the airways. However, we and others have demonstrated the presence of pre-existing T cells that recognize SARS-CoV-2 in the lower airways or oropharyngeal lymphoid tissue of unexposed individuals respectively[14, 15], likely induced by seasonal coronavirus infections. Presence of SARS-CoV-2 specific T cells were also reported in human nasal[16], lung mucosa and lung-associated lymph nodes following SARS-CoV-2 infection[17, 18]. Furthermore, increased numbers of global $CD4^+$ and $CD8^+$ in the airways of SARS-CoV-2-infected patients were associated with reduced disease severity[19, 20]. It has also been reported that spike-specific memory B cells were enriched in the lungs and associated lymph nodes of convalescent organ donors[18] and that SARS-CoV-2-binding IgA antibodies are produced more rapidly than IgG and can be detected in the serum and saliva of COVID-19 patients up to 40 days post onset of symptoms [21, 22, 23, 24].

Recent animal work with different SARS-CoV-2 vaccine formulations showed the need for mucosal immunisation to generate resident virus-specific B and T cells in the lungs and confirmed the importance of localised mucosal immunity in control of infection[17, 25, 26, 27]. Human studies that described the effect of peripheral SARS-CoV-2 vaccines on the

bioRxiv preprint doi: https://doi.org/10.1101/2023.01.25.525485; this version posted January 25, 2023. The copyright holder for this preprint (which was not certified by peer review) is the author/funder, who has granted bioRxiv a license to display the preprint in perpetuity. It is made available under aCC-BY-ND 4.0 International license.

33 respiratory mucosa are conflicting. While nasal and salivary IgA responses[28], as well as $CD4^+$
34 and $CD8^+$ T_{RM} were detected in the nasal mucosa[29] of vaccinated individuals without history
35 of SARS-CoV-2 infection[28], other studies reported minimal or lack of humoral and T cell
36 responses in nasal and lung mucosa following peripheral vaccination only[17, 30]. However,
37 such responses were detected in convalescent donors or after breakthrough infection[17, 18,
38 30, 31].
39 Further studies are needed to better characterise immune responses in the airways after
40 infection and/or vaccination and dissect out the influence of hybrid immunity, vaccine type,
41 disease severity, and particularly time since vaccination or infection to address persistence
42 of mucosal immunity. Using bronchoalveolar lavage (BAL) samples collected before the
43 onset of the COVID-19 pandemic, we have previously demonstrated that SARS-CoV-2-cross-
44 reactive T cells can reside in human airways[14]. Here, we tested BAL samples and paired
45 blood from vaccinated donors with or without prior SARS-CoV-2 infection and pre-pandemic
46 control samples. We examined the presence of peripheral and mucosal antibodies and
47 virus-specific B and T cell responses. Spike-specific B cells were detected in the airways of
48 individuals exposed to SARS-CoV-2 up to 11 months previously and virus-specific $CD4^+$ and
49 $CD8^+$ T cells were more abundant in this group compared to vaccinated uninfected
50 individuals. A better understanding of the breath and longevity of adaptive immunity to
51 SARS-CoV2 in the airways will allow us to harness protective mucosal immunity to inform
52 next generation of SARS-CoV-2 vaccines with potential to block infection and population
53 transmission.
54
55 **RESULTS**
56 **Characteristics of study groups**
57 To assess humoral and cellular immune responses in the lung mucosa and blood following
58 SARS-CoV-2 vaccination and hybrid immunity, we collected bronchoalveolar lavage (BAL)
59 fluid and paired blood samples from 7 vaccinees with no history or evidence of SARS-CoV-2
60 infection (naïve, vaccinated group) and 15 vaccinees who had serologically-confirmed
61 asymptomatic infection or experienced symptomatic infection between 2 to 11 months (56
62 – 333 days) prior to receiving SARS-CoV-2 vaccination. Vaccinated individuals with
63 asymptomatic and symptomatic infection were combined in one ‘hybrid immunity’ group,
64 due to the lack of obvious difference in immune responses to SARS-CoV-2 antigens. All

bioRxiv preprint doi: https://doi.org/10.1101/2023.01.25.525485; this version posted January 25, 2023. The copyright holder for this preprint (which was not certified by peer review) is the author/funder, who has granted bioRxiv a license to display the preprint in perpetuity. It is made available under aCC-BY-ND 4.0 International license.

65 vaccinated individuals received two doses of either mRNA or adenoviral vector vaccine. We
66 also included a pre-pandemic group (n=11) of unexposed, unvaccinated individuals as
67 controls (Figure 1A). Table 1 summarizes the demographic characteristics of the three study
68 groups and the time of sample collection in relation to infection or last vaccination.
69

70 **Airway antibody responses following hybrid immunity or vaccination alone**

71 Levels of circulating and mucosal antibodies against spike (S), receptor binding domain
72 (RBD) and nucleocapsid (N) protein were measured in serum and BAL samples in all three
73 study groups. Antibody responses to N protein (non-vaccine protein) were used to confirm
74 absence of past infection in the vaccinated cohort and classify the groups. Limit of sensitivity
75 (LOS) was set as median + 2 x standard deviation (SD) of the results in unexposed (pre-
76 pandemic) donors. As expected, anti-N IgG was below or near the LOS in the naïve
77 vaccinated group, whereas in the infected vaccinated group, it was detected in all
78 individuals (15/15) in serum and in 47% (7/15) in the BAL fluid (Extended Data Figure 1A and
79 B).

80 SARS-CoV-2 vaccination elicited robust systemic IgG responses to both S and RBD protein,
81 with levels being more pronounced in the infected vaccinated group (3.4-fold and 3.3-fold
82 median increase of anti-S and anti-RBD IgG compared to naïve vaccinated group,
83 respectively) (p=0.039) and p=0.11, respectively) (Figure 1B and C). Such systemic antibody
84 differences as a result of hybrid immunity have been extensively demonstrated in large
85 cohort vaccination studies [32, 33]. High levels of anti-S and -RBD IgG were also detected in the
86 BAL fluid of SARS-CoV-2 vaccinees. Importantly, anti-S and anti-RBD IgG levels in the lung
87 were also significantly elevated in the hybrid immunity group compared to the naïve
88 vaccinated group (8.2-fold and 9.4-fold increase for S and RBD, respectively) (p=0.024 and
89 p=0.014, respectively) (Figure 1D and E).

90 As IgA plays a crucial role in the antiviral immune defence in mucosal surfaces [34, 35], IgA
91 responses against SARS-CoV-2 proteins were also assessed in BAL samples. In the naïve
92 vaccinated group, mucosal IgA levels against S, RBD and N did not differ from the control
93 group. However, the infected vaccinated group had significantly greater mucosal anti-S IgA
94 (2.5-fold increase from control, p=0.014) and a trend to higher anti-RBD IgA (Figure 1F and
95 G), whereas the majority had non- detectable anti-N IgA levels in BAL (Extended Data Figure
96 1C).

bioRxiv preprint doi: https://doi.org/10.1101/2023.01.25.525485; this version posted January 25, 2023. The copyright holder for this preprint (which was not certified by peer review) is the author/funder, who has granted bioRxiv a license to display the preprint in perpetuity. It is made available under aCC-BY-ND 4.0 International license.

97 Vaccine-induced antibody responses to S protein demonstrated a strong correlation
98 between serum and BAL for IgG and slightly less so for IgA (Extended Data figure 1D and E).
99
100

101 **Presence of SARS-CoV-2 specific memory B cells in the lung following hybrid immunity**

102 Memory B cells are critical for long-term humoral immunity. To identify SARS-CoV-2 specific
103 memory B cells (MBCs), fluorescently labelled S, RBD and N proteins were used to assay
104 PBMCs and lung leukocytes (Figure 2A) (see gating strategy, Extended Data Figure 2A). As
105 expected, and in line with the antibody responses, only vacinees who had previously been
106 exposed to viral nucleoprotein through infection had detectable N-specific MBCs in the
107 blood. By contrast, both naïve vaccinated and infected vaccinated individuals had
108 circulating S- and RBD-specific MBCs above the background staining threshold (set as
109 median + 2 x SD of pre-pandemic levels).
110 B cells are an underrepresented cell population in the lung mucosa; their presence in the
111 lung is usually associated with infection or chronic inflammation[36]. Although data on anti-
112 viral B cell immunity in human respiratory mucosa are scarce, murine model studies of
113 influenza infection demonstrated the generation of flu-specific memory B cells in the lung
114 following influenza infection that were able to produce more antibodies with enhanced
115 potential to recognise viral variants[4, 5, 6]. In this study, the small number of B cells in the BAL
116 samples allowed the assessment of SARS-CoV-2 specific MBCs only in the hybrid immunity
117 group. The frequencies of S-, RBD- and N-specific MBCs were greater in the lung mucosa of
118 infected vaccinated individuals compared to pre-pandemic controls (median 5.5% vs 0.08%
119 for S, 2.88% vs 0.06% for RBD and 1.69% vs 0.06% for N-specific responses (p=0.0004,
120 p=0.016 and p=0.016, respectively) (Figure 2E-2G). Paired sample comparison of the
121 frequencies of circulating and mucosally detected anti-viral MBCs in the infected vaccinated
122 group revealed enrichment of S- and RBD-specific MBCs in the lung mucosa. The median
123 frequencies of S- and RBD-specific MBCs were 2.1-fold (p=0.0078) and 3.8-fold (p=0.062)
124 higher in the BAL compared to PBMC sample from the same donors (Figure 2H). We
125 detected that in the lung mucosa memory B cells were mainly class-switched MBCs,
126 whereas paired blood samples had a significantly increased proportion of unswitched MBCs
127 cells (Figure 2I).

bioRxiv preprint doi: https://doi.org/10.1101/2023.01.25.525485; this version posted January 25, 2023. The copyright holder for this preprint (which was not certified by peer review) is the author/funder, who has granted bioRxiv a license to display the preprint in perpetuity. It is made available under aCC-BY-ND 4.0 International license.

128 We also stratified the infected vaccinated group based on the vaccine they received. Despite
129 the small sample size, mRNA vaccinated individuals exhibited 1.8-fold higher frequency of
130 circulating S-specific MBCs compared to ChAdOX1_S recipients (p=0.037), and a trend to
131 higher RBD-specific B cells (Extended Data Figure 2B). In lung mucosa, a similar trend was
132 observed for S-specific MBCs levels (Extended Data Figure 2C), but low cell yields hindered a
133 robust analysis.
134

135 **Robust T cells responses in the lung mucosa after infection and vaccination but not**
136 **vaccination alone**

137 Circulating and tissue resident memory (T_{RM}) T cells are important in constraining viral
138 spread and protect against severe disease when neutralising antibodies fail to confer
139 sterilising immunity[37, 38, 39]. Moreover, we showed that T cells targeting the early expressed
140 replication transcription complex (RTC: NSP7,12,13) are selectively associated with infection
141 being aborted before detection by PCR or seroconversion and can be detected in pre-
142 pandemic blood and lung samples[14, 40]. Therefore, we examined T cell responses in blood
143 and BAL samples following vaccination alone or infection and vaccination in blood and
144 paired BAL samples.
145 The frequencies of circulating and lower airway $CD4^+$ and $CD8^+$ T cells were measured based
146 on the expression of activation-induced markers (AIM assay) after stimulation with SARS-
147 CoV-2 peptides (for full gating strategy see Extended Data figure 3A) and were compared to
148 pre-existing cross-reactive responses detectable using the same assays in cryopreserved
149 pre-pandemic BAL samples. BAL samples were further divided by the expression of
150 prototypic tissue residency markers (CD69/CD103 co-expression for CD8 and CD69/CD49a
151 expression for CD4/CD49a into T_{RM} and recirculating T cells. As reported by others[41, 42, 43],
152 SARS-CoV-2 vaccination alone induced notable S-specific $CD4^+$ and $CD8^+$ T cell responses in
153 the circulation when compared to pre-pandemic controls (Figure 3B and 3C). In the infected
154 vaccinated group, the frequency of circulating S-specific $CD4^+$ and $CD8^+$ T cells tended to be
155 higher than the naïve vaccinated group (1.8-fold and 4.8-fold increase, respectively).
156 Despite the induction of T cell immunity systemically, vaccination alone did not elicit S-
157 specific T cell responses that were significantly greater than those in pre-pandemic samples
158 within the global (Figure 3D and 3E) or T_{RM} lung compartment (Figure 3F and 3G).

bioRxiv preprint doi: https://doi.org/10.1101/2023.01.25.525485; this version posted January 25, 2023. The copyright holder for this preprint (which was not certified by peer review) is the author/funder, who has granted bioRxiv a license to display the preprint in perpetuity. It is made available under aCC-BY-ND 4.0 International license.

159 As opposed to vaccination alone, BAL samples from those who acquired hybrid immunity
160 exhibited greater anti-Spike T cell responses than either the pre-pandemic or naïve
161 vaccinated group (Figure 3D-3G). Within the global T cell population, the frequency of S-
162 specific $CD4^+$ and $CD8^+$ T cells increased by 2.8-fold and 5.3-fold higher in the infected,
163 vaccinated group compared to the naïve, vaccinated group (p=0.048 and p=0.012,
164 respectively) (Figure 3D and 3E). A similar profile was observed in the T_{RM} T cell
165 compartment, with S-specific $CD4^+$ and $CD8^+$ T cell frequencies being 2.8-fold and 4.8-fold
166 greater, respectively, in the hybrid immunity group compared to naïve vaccinated group
167 (p=0.05 and p=0.017, respectively) (Figure 3F and 3G). In addition, within the global T cell
168 population, the frequencies of S-specific $CD4^+$ and $CD8^+$ T cells were substantially higher in
169 BAL than in paired blood from infected vaccinated individuals (median 2.45% vs 0.62% of S-
170 specific $CD4^+$ T cells and median 1.84% vs 0.24% of S-specific $CD8^+$ T in BAL and paired blood
171 of infected, vaccinated individual, respectively) (p=0.0005 and p=0.0002, respectively)
172 (Figure 3H and 3I). In the naïve, vaccinated group the frequency of S-specific $CD4^+$ but not
173 $CD8^+$ T cells was slightly higher in BAL than PBMCs (median 0.89% vs 0.35% in BAL and
174 paired blood, respectively).
175
176 In agreement with large vaccination studies[44, 45], we observed that adenoviral vector vaccine
177 tended to induce increased frequency of S-specific T cells in the periphery compared to
178 mRNA vaccines. The tendency of the adenoviral vector vaccine to induce stronger T cell
179 immunity was also observed in the lower airways, with 3.3-fold and 2.5-fold higher S-
180 specific $CD4^+$ and $CD8^+$ T cell responses when compared to RNA vaccination (Extended Data
181 Figure 3B-C).
182
183 We also examined T cell specificities for non-vaccine included SARS-CoV-2 structural
184 proteins (N and membrane [M]) and non-structural proteins (NSP-7, NSP-12 and NSP-13
185 pool, representative of the core replication-transcription complex [RTC]) in blood and BAL
186 (Extended Data Figure 3D-E and Figure 4). As expected, the frequencies of circulating N- and
187 M-specific $CD4^+$ and $CD8^+$ T cells were significantly higher than in pre-pandemics only in the
188 hybrid immunity group, as those vaccinees had a past SARS-CoV-2 infection (Figure 4A and
189 4B). In the case of RTC-specific T cells, their frequency did not differ amongst groups, as
190 SARS-CoV-2 cross-reactive $CD4^+$ and $CD8^+$ T cell responses were detected systemically in 3

bioRxiv preprint doi: https://doi.org/10.1101/2023.01.25.525485; this version posted January 25, 2023. The copyright holder for this preprint (which was not certified by peer review) is the author/funder, who has granted bioRxiv a license to display the preprint in perpetuity. It is made available under aCC-BY-ND 4.0 International license.

191 out 8 pre-pandemic controls, in line with previous studies[14, 40, 46]. In BAL samples, the
192 frequency of the aforementioned T cell specificities was tested in a subset of pre-pandemic
193 and infected, vaccinated individuals based on cell number availability. Interestingly, the
194 hybrid immunity group had, or tended to have, higher N- and M- and RCT-specific T cell
195 responses within the global and TRM T cell compartment in BAL samples compared to levels
196 detected in pre-pandemic controls (Figure 4C-4F). In addition, these SARS-CoV-2 specific
197 $CD4^+$ and $CD8^+$ T cell responses were enriched in the lower airways compared to the
198 periphery (Figure 4G and 4H).
199
200 The hierarchy of SARS-CoV-2 antigen recognition by circulating and lower airway T cells of
201 each distinct peptide pool (S, N, M and RTC) was analysed in a subset of 8 infected
202 vaccinated individuals (Extended Data Figure 3D-E). The antigen recognition profile differed
203 between systemic and airway localised T cells, and between T cell subsets. SARS-CoV-2
204 specific $CD4^+$ T cells were largely dominated by S-specific $CD4^+$ T cells in the periphery and
205 lung mucosa, however in lower airway they were enriched with additional T cell specificities
206 (Extended Data figure 3D). In the case of SARS-CoV-2 $CD8^+$ T cells, their antigen recognition
207 profile was more diverse in both sites, with S-specific $CD8^+$ T cells being apparent but not
208 dominant (Extended Data figure 3E).
209

210 **Longevity of antibody and T cells responses in lung mucosa following vaccination alone or**
211 **hybrid immunity**

212 To assess the longevity of vaccine-induced SARS-CoV-2 immune memory in the lung mucosa
213 following vaccination and hybrid immunity, antibody and T cell responses assessed in BAL
214 and paired blood of naïve, vaccinated and infected vaccinated individuals were plotted in
215 association with time post the 2nd vaccine dose (which was 2-11 months after any known
216 infection dates). Levels of circulating anti-S and anti-RBD IgG were negatively correlated
217 with time post-vaccination in the naïve vaccinated but not the infected vaccinated group,
218 implying quicker antibody decay in the naïve vaccinated donors (Figure 5A). In the lung
219 mucosa, anti-S and anti-RBD IgG levels exhibited similar rates of decay between the two
220 vaccinated groups (Figure 5B). On the other hand, levels of anti-S and RBD IgA in BAL were
221 detectable only following hybrid immunity but they quickly reached pre-pandemic levels (at
222 5-months post-vaccination, Figure 4C). This result is in agreement with previous studies in

bioRxiv preprint doi: https://doi.org/10.1101/2023.01.25.525485; this version posted January 25, 2023. The copyright holder for this preprint (which was not certified by peer review) is the author/funder, who has granted bioRxiv a license to display the preprint in perpetuity. It is made available under aCC-BY-ND 4.0 International license.

223 convalescent patients that reported short-lived IgA-mediated immunity at mucosal sites[21,
224 47].
225
226 Circulating and lower-airway S-specific T cell frequencies were also plotted in association
227 with time post-vaccination in both vaccinated groups. In blood, numbers of S-specific $CD4^+$
228 and $CD8^+$ T cells declined over time in the infected vaccinated group and at 5-months post-
229 vaccination reached the frequencies induced by vaccination alone (Figure 6A). On the other
230 hand, S-specific T cell responses were better sustained in the lung mucosa following hybrid
231 immunity. Despite a trend of negative association with time post-vaccination, S-specific
232 $CD4^+$ T cell responses were detectable from the lung mucosa of infected vaccinated
233 individuals for over 5-months post vaccination. Lower-airway S-specific $CD8^+$ T cells did not
234 associate negatively with time, suggesting they remained at stable levels throughout the
235 period of 5-months post vaccination (Figure 6B and 6C). The human lung also retained
236 partial immune memory to SARS-CoV-2 over a year post infection. Despite decline over
237 time, T cell specificities not affected by SARS-CoV-2 vaccination, such as M-, N- and RTC-
238 specific $CD4^+$ and $CD8^+$ T cells, were detectable in various frequencies between 6 to 18
239 months post infection (Figure 6D), rendering these conserved SARS-CoV-2 proteins as
240 potential vaccine targets.
241
242
243 **DISCUSSION**
244 Despite high SARS-CoV-2 seroprevalence globally by either vaccination or infection, regular
245 waves continue to cause breakthrough infections. Immunological memory to SARS-CoV-2 in
246 the respiratory mucosa following vaccination, infection and hybrid immunity is not well
247 understood. Protective mucosal immunity could be harnessed for the development of
248 vaccines specifically targeting protection against airway infection to block transmission of
249 the virus in the population.
250
251 Here, we assessed the potential of peripheral SARS-CoV-2 vaccination to induce anti-viral
252 immune memory in the human lung mucosa and whether a prior infection would influence
253 the immunological outcome. We found that following SARS-CoV-2 vaccination alone the
254 lung mucosa was enriched with spike IgG, but levels were increased and accompanied by

bioRxiv preprint doi: https://doi.org/10.1101/2023.01.25.525485; this version posted January 25, 2023. The copyright holder for this preprint (which was not certified by peer review) is the author/funder, who has granted bioRxiv a license to display the preprint in perpetuity. It is made available under aCC-BY-ND 4.0 International license.

255 mucosal IgA in the setting of hybrid immunity. Importantly, homologous parenteral SARS-
256 CoV-2 vaccination (mRNA or adenoviral vector vaccine) did not seed the human lung with
257 tissue-residing spike-specific T cells, despite the induction of notable T cell responses in the
258 circulation. Compared to SARS-CoV-2 vaccination alone, hybrid immunity resulted in
259 considerably higher humoral and cellular immune responses against the vaccine antigens in
260 the periphery. In contrast to vaccination alone, hybrid immunity generated robust and
261 persistent spike-specific T cell immunity in the human lung mucosa, complemented with
262 local MBC and T cell responses against additional SARS-CoV-2 antigens. A long-lived, airway-
263 compartmentalised B and T cell reservoir in the lung mucosa may confer better recognition
264 of Omicron sublineages and future variants and protect against severe disease, supporting
265 the need for vaccines specifically targeting the airways.
266
267 In line with others[17, 31], our results indicate that following vaccination alone, SARS-CoV-2
268 immunity in the respiratory mucosa is limited to humoral immunity, with IgG dominating
269 over IgA titres against the vaccine-antigens. Induction of both anti-Spike IgG and IgA was
270 more efficient in the lung mucosa of vaccinated individuals with prior infection. The strong
271 correlation observed between anti-S IgG in serum and BAL samples supports the notion that
272 systemic antibodies elicited by vaccination transudate to the respiratory mucosa, as
273 previous vaccination studies have reported[48, 49]. Despite the key role of antibodies in
274 neutralising the virus at the respiratory mucosa- the primary site of infection, local humoral
275 immunity wanes quickly[21] making individuals more susceptible to immune escape by
276 Omicron sublineages and future variants[17]. In addition, findings from other respiratory
277 infection and vaccination studies indicate that higher levels of antibodies are required in the
278 nasal mucosa to protect against local infection compared to levels required in blood to
279 protect against invasive disease [50]. However, the finding of class-switched memory B cells
280 enriched in the lung mucosa raises the possibility they produce a repertoire of antibodies
281 better able to cross-recognise variants, as shown in other infections[4]. Mucosal antibodies
282 may also harness local lung cells such as NK cells and phagocytes for non-neutralising Fc-
283 dependent cellular immunity.
284
285 Booster parenteral vaccination is required to enhance waning humoral immunity, but the
286 frequency and intensity of robust systemic T-cell responses is not boosted by the additional

bioRxiv preprint doi: https://doi.org/10.1101/2023.01.25.525485; this version posted January 25, 2023. The copyright holder for this preprint (which was not certified by peer review) is the author/funder, who has granted bioRxiv a license to display the preprint in perpetuity. It is made available under aCC-BY-ND 4.0 International license.

287 vaccination[51]. Hybrid immunity elicits considerably high humoral and cellular responses in
288 the periphery, which exceed the immune responses induced solely by vaccination[32, 52, 53].
289 Studying the human lung mucosa, we provide the first evidence, to our knowledge, that
290 hybrid immunity, contrary to SARS-CoV-2 immunisation alone, can generate robust,
291 broader, and long-lived anti-viral immune responses in the lower airways. In line with other
292 studies[17, 18], the intensity of S-specific B and T cell responses were enriched in the lung
293 mucosa compared to the periphery and similarly, enriched B and T cells responses were
294 detected for other SARS-CoV-2 antigens. These lower-airway localised B and T cells
295 reservoirs were long-lived. Hence using more comprehensive analysis of T cell specificities,
296 we demonstrated that lower airway T cell immunity against SARS-CoV-2 can be sustained
297 for over a year post the initial exposure to the pathogen. In studies of other respiratory
298 viruses, lung localised, tissue-residing B and T cells associate with protection in mouse
299 models of influenza[5, 54] and RSV infection[10]. In human challenge models of influenza and RSV
300 infection, enrichment of $CD4^+$ and $CD8^+$ T_{RM} cells in the airways was associated with
301 mitigated respiratory symptoms, viral control, and reduced disease severity[12, 55]. The
302 prolonged memory together with the ability of T cells to better recognise more conserved
303 parts of SARS-CoV-2, support the utility of developing multi-specific mucosally-administered
304 vaccines that could boost tissue localised and resident memory T and B cells in the lung.
305 Preclinical studies of SARS-CoV-2 have demonstrated that intranasal vaccination decreases
306 viral shedding and transmission relative to parenteral vaccines[27, 56, 57]. In addition, the
307 combined approach of systemic priming SARS-CoV-2 vaccination followed by intranasal
308 boosting with either adenovirus vectored vaccines or an adjuvanted Spike vaccine elicited
309 both systemic and protective mucosal immunity with cross-reactive properties[58, 59]. In
310 humans, there are limited data on the immunogenicity of SARS-CoV-2 vaccines that target
311 the airways, focusing mainly on humoral immunity[60].
312
313 Our study has limitations. Due to the invasive nature of the bronchoscopy procedure, we
314 were not able to recruit a large cohort of study participants. In addition, the fast roll out and
315 uptake of COVID-19 vaccine programme in the UK hindered the recruitment of convalescent
316 unvaccinated individuals. The low BAL cell yields restricted the analysis of other T cell
317 specificities to selected SARS-CoV-2 proteins and did not allow the assessment of vaccine-
318 induced memory B cells in the lung mucosa of infection naïve individuals. Given the inability

bioRxiv preprint doi: https://doi.org/10.1101/2023.01.25.525485; this version posted January 25, 2023. The copyright holder for this preprint (which was not certified by peer review) is the author/funder, who has granted bioRxiv a license to display the preprint in perpetuity. It is made available under aCC-BY-ND 4.0 International license.

319 of SARS-CoV-2 parenteral immunisation to generate tissue-localised T cell immunity, it is
320 less likely that S-specific memory B cells will be present in the lung mucosa following
321 vaccination. Although, we were able to detect and characterise T cell specificities for over a
322 year post infection and up to 6 months post vaccination, future longitudinal studies are
323 needed to fully understand the long-term impact of airway localised T and B cell immunity in
324 SARS-CoV-2 protection.
325
326 Overall, our data suggest robust lung mucosal immunity against SARS-CoV-2 can be better
327 achieved through hybrid immunity, as opposed to peripheral vaccination alone. Vaccines
328 that induce airway localised memory T and B cells may provide broader long-term
329 protection at the site of infection. Thus, vaccination approaches that combine systemic and
330 mucosal immunisation could reduce virus transmission and re-infection cases.
331

332 **METHODS**

333 **Study design and cohorts**

334 This was a cross-sectional study, which included a cohort of SARS-CoV-2 vaccinated
335 individuals (n=22), who had received two doses of mRNA or the ChAdOx1_S adenoviral
336 vector vaccine. A subset of them had experienced PCR-confirmed symptomatic infection
337 (n=12) or serologically confirmed asymptomatic infection (n=3), referred to the group of
338 infected and vaccinated individuals (hybrid immunity) (n=15), whereas the remaining
339 vaccinees had not experienced SARS-CoV-2 infection (vaccinated, n=7). BAL samples were
340 obtained through research bronchoscopy 1 to 6 months (23-186 days) after the 2nd vaccine
341 dose and 7 to 19 months (201 -570 days) after symptoms onset for those who had
342 experienced COVID-19. These COVID-19 convalescent individuals had been admitted to
343 hospital between April 2020 to January 2021, when the ancestral SARS-CoV-2 strain was still
344 dominant in the UK. Blood samples for sera and PBMC isolation were collected at the same
345 day as BAL. Pre-pandemic samples from healthy, unexposed individuals (n=11), collected
346 from 2015 to 2018, were also included into the analysis, as a control group (Figure 1A). The
347 demographic and clinical characteristics of the 3 study groups are shown in Table 1.

348 **Sample processing**

bioRxiv preprint doi: https://doi.org/10.1101/2023.01.25.525485; this version posted January 25, 2023. The copyright holder for this preprint (which was not certified by peer review) is the author/funder, who has granted bioRxiv a license to display the preprint in perpetuity. It is made available under aCC-BY-ND 4.0 International license.

349 BAL samples were processed as previously described[61], cryopreserved in CTL-CryoABC
350 medium kit (Immunospot). After thawing, alveolar macrophages were routinely separated
351 from other non-adherent immune cell populations using an adherence step, as previously
352 described[62]. Blood was processed for sera collection or PBMCs were isolated from
353 heparinized blood samples using density-gradient sedimentation layered over Ficoll-Paque
354 in SepMate tube and then cryopreserved in CTL-CryoABC medium kit (Immunospot).

355 **ELISA for SARS-CoV-2 proteins**

356 ELISA was used to quantify levels of IgG and IgA against Spike trimer, RBD and N in serum
357 and BAL samples, as previously described[63]. Briefly, 96-well plates (U bottom) were coated
358 with 1µg/ml SARS-CoV-2 antigen and stored at 4°C overnight for at least 16h. The next day,
359 plates were washed 3 times with PBS/0.05% Tween-20 and blocked with 2% BSA in PBS for
360 1h at room temperature. Sera and BAL diluted in 0.1% BSA-PBS were plated in duplicate and
361 incubated for 2h at room temperature alongside an internal positive control (dilution of a
362 convalescent serum) to measure plate to plate variation. For the standard curve, a pooled
363 sera of SARS-CoV-2 infected participants was used in a two-fold serial dilution to produce
364 either eight or nine standard points (depending on the antigen) that were assigned as
365 arbitrary units. Goat anti-human IgG (γ-chain specific, A9544, Millipore-Sigma) or IgA (α-
366 chain specific, A9669, Millipore-Sigma) conjugated to alkaline phosphatase was used as
367 secondary antibody, and plates were developed by adding 4-nitrophenyl phosphate in
368 diethanolamine substrate buffer. Optical densities were measured using an Omega
369 microplate reader at 405nm. Blank corrected samples and standard values were plotted
370 using the 4-Parameter logistic model (Gen5 v3.09, BioTek).
371

372 **B cells immunophenotyping and detection of SARS-CoV-2 specific B cells**

373 Cryopreserved BAL cells and PBMCs were used for detection of SARS-CoV-2 specific B cells in
374 lower airways and blood, respectively. Biotinylated tetrameric S, RBD and N protein were
375 individually labelled with different streptavidin conjugates at 4°C for 1h, as previously
376 described[63].
377 Biotinylated S and RBD were directly labelled with Streptavidin-PE (with a ratio 1:3 and 1:
378 5.7, respectively); with Streptavidin-BV570 (S with a ratio 1: 2.7); and Streptavidin-BV785

bioRxiv preprint doi: https://doi.org/10.1101/2023.01.25.525485; this version posted January 25, 2023. The copyright holder for this preprint (which was not certified by peer review) is the author/funder, who has granted bioRxiv a license to display the preprint in perpetuity. It is made available under aCC-BY-ND 4.0 International license.

379 (RBD with a ratio 1:5). Biotinylated N protein was labelled with Streptavidin-PE (with a ratio
380 of 1:2.3) and Streptavidin-AF647 (N protein with a ratio 1: 0.5).
381 PBMCs and BAL cells were thawed and stained with Live/dead e506 viability dye and an
382 antibody cocktail for surface markers for 30min in the dark, washed twice and resuspended
383 in 200µL of PBS. Parallel samples stained with an identical panel of monoclonal antibodies
384 (mAbs),but excluding the SARS-CoV-2 proteins (fluorescence minus one [FMO] controls),
385 were used as controls for nonspecific binding. All samples were acquired on an Aurora
386 cytometer (Cytek Biosciences) and analysed with Flowjo software version 10 (Treestar). The
387 flow-cytometry panel of mAbs used to phenotype global and antigen-specific subsets can be
388 seen in Supplementary Table 1.
389 The frequency of antigen-specific B cells was calculated within the fraction of MBCs
390 ($CD19^+CD27^+$, excluding the naïve IgD^+CD27^- and the double negative IgG^-CD27^- fractions,
391 see gating strategy (Extended Data Figure 2A). For phenotypic analysis of spike-, RBD-, and
392 N-specific B cells, a sufficient magnitude of responses (≥50 cells in the relevant parent gate)
393 was required.
394

395 **Activation-induced markers (AIM) T cell assay**

396 Mononuclear BAL cells (1 x 10^5 cells per well) and PBMCs (1 x 10^6 cells per well) were
397 seeded in 96-well plates in RPMI supplemented with 1% PNS and 10% AB human serum
398 (Merck, UK) and stimulated with SARS-CoV-2 specific peptides pools. The peptides pools
399 used were spanning the whole Spike protein based on predicted epitopes (15-mer peptides
400 overlapping by 10 amino acids)[64] or overlapping peptides spanning the immunogenic
401 domains of the SARS-CoV-2 N (Prot_N) and M (Prot_M) purchased from Miltenyi Biotec[63] or
402 combined pools spanning SARS-CoV-2 NSP7, NSP12 and NSP13 proteins (15-mer peptides
403 overlapping by 10 amino acids) of the ancestral SARS-CoV-2 strain[14, 65]. Prior to the peptide
404 addition, cells were blocked with 0.5µg/ml of anti-CD40 mAb (Miltenyi Biotec) for 15min at
405 37°C. A stimulation with an equimolar amount of DMSO was performed as a negative
406 control and Staphylococcal enterotoxin B (SEB, 2 µg/mL) was included as a positive control.
407 The following day cells were harvested from plates, washed and stained for surface markers
408 (Supplemental table 2 and 3).
409 AIM^+ $CD4^+$ T cells were identified as $CD40L^+OX40^+$, $4\text{-}1BB^+OX40^+$, $4\text{-}1BB^+CD40L^+$ subsets, and
410 the $CD40L^+OX40^+$ combination was used to quantify SARS-CoV-2 specific $CD4^+$ T cells

bioRxiv preprint doi: https://doi.org/10.1101/2023.01.25.525485; this version posted January 25, 2023. The copyright holder for this preprint (which was not certified by peer review) is the author/funder, who has granted bioRxiv a license to display the preprint in perpetuity. It is made available under aCC-BY-ND 4.0 International license.

411 frequency. SARS-CoV-2 specific $CD8^+$ T cells were identified as 4-$1BB^+CD25^+$. Antigen-specific
412 $CD4^+$ and $CD8^+$ T cells were measured and presented as DMSO background–subtracted data.
413

414 **Statistical analysis**

415 Participant characteristics were summarised as n, median (interquartile range) or frequency
416 (percentage). Chi-squared test and Fisher's exact test were conducted to identify any
417 significant changes in categorical variables. Non-parametric Wilcoxon paired tests and
418 Mann-Whitney tests were conducted to compare quantitative data within the same group
419 or between two groups, respectively. In addition, Kruskal-Wallis rank sum test with Dunn's
420 correction were performed to compare quantitative data amongst groups (three groups
421 comparison). All tests were two-sided with an α level of 0.05. To explore the association
422 between time after infection and vaccination, we employed a linear regression model. Data
423 were analysed in R software version 4.0.3 (R Foundation for Statistical Computing, Vienna,
424 Austria) or Graphpad Prism version 9.0.
425

426 **Ethics statement**

427 All volunteers gave written informed consent and research was conducted in compliance
428 with all relevant ethical regulations. Ethical approval was given by the NorthWest National
429 Health Service Research Ethics Committee (REC no. 18/NW/0481 and Human Tissue
430 licensing no. 12548).
431

432 **Acknowledgements**

433 We thank all the patients and healthy volunteers who participated in the present study and
434 all the clinical staff who helped with recruitment and sample collection. The study was
435 financially supported by EPSRC grant (no. EP/W016389/1) awarded to E.M and D.M.F and a
436 Centre of Excellence in Infectious Diseases Research (CEIDR) pump-priming grant. Collection
437 of pre-pandemic clinical samples was supported by the Bill and Melinda Gates Foundation
438 (grant no. OPP1117728) and the UK Medical Research Council (grant no. M011569/1)
439 awarded to D.M.F. The production of peptide pools has been funded or in part with federal
440 funds from the National Institutes of Health, Contract No. 75N9301900065 to A.S, D.W.
441 M.K.M. is supported by Wellcome Trust Investigator Award (no. 214191/Z/18/Z) and CRUK
442 Immunology grant (no.26603).

bioRxiv preprint doi: https://doi.org/10.1101/2023.01.25.525485; this version posted January 25, 2023. The copyright holder for this preprint (which was not certified by peer review) is the author/funder, who has granted bioRxiv a license to display the preprint in perpetuity. It is made available under aCC-BY-ND 4.0 International license.

443

444 **Authors contribution**

445 E.M, M.O.D, M.K.M and D.M.F conceived and designed the study. A.H.W and M.F recruited
446 and consented study participants. A.H.W, M.F, R.R and A.M.C obtained human samples.
447 E.M, J.R, J.H and CS processed samples. E.M, M.O.D, J.R, J.H, O.O and T.L generated and
448 analysed the data. E.M. M.O.D, M.K.M and D.M.F interpreted data. E.M, J.R and B.U
449 developed the assays. S.J.D, D.W and A.S provided material for the assays. E.M and M.O.D
450 prepared the manuscript. All authors provided critical input into the manuscript.

451

452 **Declaration of Interest**

453 A.S. is a consultant for Gritstone Bio, Flow Pharma, Moderna, AstraZeneca, Qiagen, Fortress,
454 Gilead, Sanofi, Merck, RiverVest, MedaCorp, Turnstone, NA Vaccine Institute, Emervax,
455 Gerson Lehrman Group and Guggenheim. LJI has filed for patent protection for various
456 aspects of T cell epitope and vaccine design work.

457

REFERENCES

458 1. Zheng, M.Z.M. & Wakim, L.M. Tissue resident memory T cells in the respiratory tract.
459 *Mucosal Immunology* (2021).
460
461 2. Son, Y.M. & Sun, J. Co-Ordination of Mucosal B Cell and CD8 T Cell Memory by
462 Tissue-Resident CD4 Helper T Cells. *Cells* **10** (2021).
463
464 3. Lee, C.M. & Oh, J.E. Resident Memory B Cells in Barrier Tissues. *Front Immunol* **13**,
465 953088 (2022).
466
467 4. Adachi, Y. *et al.* Distinct germinal center selection at local sites shapes memory B cell
468 response to viral escape. *J Exp Med* **212**, 1709-1723 (2015).
469
470 5. Allie, S.R. *et al.* The establishment of resident memory B cells in the lung requires
471 local antigen encounter. *Nature Immunology* **20**, 97-108 (2019).
472
473 6. Onodera, T. *et al.* Memory B cells in the lung participate in protective humoral
474 immune responses to pulmonary influenza virus reinfection. *Proc Natl Acad Sci U S A*
475 **109**, 2485-2490 (2012).
476
477 7. Wu, T. *et al.* Lung-resident memory CD8 T cells (TRM) are indispensable for optimal
478 cross-protection against pulmonary virus infection. *J Leukoc Biol* **95**, 215-224 (2014).

bioRxiv preprint doi: https://doi.org/10.1101/2023.01.25.525485; this version posted January 25, 2023. The copyright holder for this preprint (which was not certified by peer review) is the author/funder, who has granted bioRxiv a license to display the preprint in perpetuity. It is made available under aCC-BY-ND 4.0 International license.

479
480 8. Pizzolla, A. *et al.* Resident memory CD8(+) T cells in the upper respiratory tract
481 prevent pulmonary influenza virus infection. *Sci Immunol* **2** (2017).
482
483 9. Turner, D.L. *et al.* Lung niches for the generation and maintenance of tissue-resident
484 memory T cells. *Mucosal Immunol* **7**, 501-510 (2014).
485
486 10. Kinnear, E. *et al.* Airway T cells protect against RSV infection in the absence of
487 antibody. *Mucosal Immunol* **11**, 249-256 (2018).
488
489 11. Luangrath, M.A., Schmidt, M.E., Hartwig, S.M. & Varga, S.M. Tissue-Resident
490 Memory T Cells in the Lungs Protect against Acute Respiratory Syncytial Virus
491 Infection. *Immunohorizons* **5**, 59-69 (2021).
492
493 12. Jozwik, A. *et al.* RSV-specific airway resident memory CD8+ T cells and differential
494 disease severity after experimental human infection. *Nat Commun* **6**, 10224 (2015).
495
496 13. Zhao, J. *et al.* Airway Memory CD4(+) T Cells Mediate Protective Immunity against
497 Emerging Respiratory Coronaviruses. *Immunity* **44**, 1379-1391 (2016).
498
499 14. Diniz, M.O. *et al.* Airway-resident T cells from unexposed individuals cross-recognize
500 SARS-CoV-2. *Nat Immunol* **23**, 1324-1329 (2022).
501
502 15. Niessl, J. *et al.* Identification of resident memory CD8(+) T cells with functional
503 specificity for SARS-CoV-2 in unexposed oropharyngeal lymphoid tissue. *Sci Immunol*
504 **6**, eabk0894 (2021).
505
506 16. Roukens, A.H.E. *et al.* Prolonged activation of nasal immune cell populations and
507 development of tissue-resident SARS-CoV-2-specific CD8+ T cell responses following
508 COVID-19. *Nature Immunology* **23**, 23-32 (2022).
509
510 17. Tang, J. *et al.* Respiratory mucosal immunity against SARS-CoV-2 after mRNA
511 vaccination. *Sci Immunol* **7**, eadd4853 (2022).
512
513 18. Poon, M.M.L. *et al.* SARS-CoV-2 infection generates tissue-localized immunological
514 memory in humans. *Sci Immunol* **6**, eabl9105 (2021).
515
516 19. Szabo, P.A. *et al.* Longitudinal profiling of respiratory and systemic immune
517 responses reveals myeloid cell-driven lung inflammation in severe COVID-19.
518 *Immunity* **54**, 797-814 e796 (2021).
519
520 20. Liao, M. *et al.* Single-cell landscape of bronchoalveolar immune cells in patients with
521 COVID-19. *Nat Med* **26**, 842-844 (2020).
522
523 21. Sterlin, D. *et al.* IgA dominates the early neutralizing antibody response to SARS-CoV-
524 2. *Science Translational Medicine* **13**, eabd2223 (2021).
525

bioRxiv preprint doi: https://doi.org/10.1101/2023.01.25.525485; this version posted January 25, 2023. The copyright holder for this preprint (which was not certified by peer review) is the author/funder, who has granted bioRxiv a license to display the preprint in perpetuity. It is made available under aCC-BY-ND 4.0 International license.

526 22. Yu, H.Q. *et al.* Distinct features of SARS-CoV-2-specific IgA response in COVID-19
527 patients. *Eur Respir J* **56** (2020).
528
529 23. Ma, H. *et al.* Serum IgA, IgM, and IgG responses in COVID-19. *Cellular & Molecular*
530 *Immunology* **17**, 773-775 (2020).
531
532 24. Seow, J. *et al.* Longitudinal evaluation and decline of antibody responses in SARS-
533 CoV-2 infection. *medRxiv*, 2020.2007.2009.20148429 (2020).
534
535 25. Oh, J.E. *et al.* Intranasal priming induces local lung-resident B cell populations that
536 secrete protective mucosal antiviral IgA. *Sci Immunol* **6**, eabj5129 (2021).
537
538 26. Afkhami, S. *et al.* Respiratory mucosal delivery of next-generation COVID-19 vaccine
539 provides robust protection against both ancestral and variant strains of SARS-CoV-2.
540 *Cell* **185**, 896-915 e819 (2022).
541
542 27. van Doremalen, N. *et al.* Intranasal ChAdOx1 nCoV-19/AZD1222 vaccination reduces
543 viral shedding after SARS-CoV-2 D614G challenge in preclinical models. *Sci Transl*
544 *Med* **13** (2021).
545
546 28. S, G. *et al.* Serological response to SARS-CoV-2 vaccination in multiple sclerosis
547 patients treated with fingolimod or ocrelizumab: an initial real-life experience. *J*
548 *Neurol* **269**, 39-43 (2022).
549
550 29. Ssemaganda, A. *et al.* Expansion of cytotoxic tissue-resident CD8+ T cells and
551 CCR6+CD161+ CD4+ T cells in the nasal mucosa following mRNA COVID-19
552 vaccination. *Nature Communications* **13**, 3357 (2022).
553
554 30. Lim, J.M.E. *et al.* SARS-CoV-2 breakthrough infection in vaccinees induces virus-
555 specific nasal-resident CD8+ and CD4+ T cells of broad specificity. *J Exp Med* **219**
556 (2022).
557
558 31. Sano, K. *et al.* SARS-CoV-2 vaccination induces mucosal antibody responses in
559 previously infected individuals. *Nature Communications* **13**, 5135 (2022).
560
561 32. Bates, T.A. *et al.* Vaccination before or after SARS-CoV-2 infection leads to robust
562 humoral response and antibodies that effectively neutralize variants. *Sci Immunol* **7**,
563 eabn8014 (2022).
564
565 33. Krammer, F. *et al.* Antibody Responses in Seropositive Persons after a Single Dose of
566 SARS-CoV-2 mRNA Vaccine. *New England Journal of Medicine* **384**, 1372-1374
567 (2021).
568
569 34. Sterlin, D. *et al.* IgA dominates the early neutralizing antibody response to SARS-CoV-
570 2. *Sci Transl Med* **13** (2021).
571

bioRxiv preprint doi: https://doi.org/10.1101/2023.01.25.525485; this version posted January 25, 2023. The copyright holder for this preprint (which was not certified by peer review) is the author/funder, who has granted bioRxiv a license to display the preprint in perpetuity. It is made available under aCC-BY-ND 4.0 International license.

572 35. Mazanec, M.B., Coudret, C.L. & Fletcher, D.R. Intracellular neutralization of influenza
573 virus by immunoglobulin A anti-hemagglutinin monoclonal antibodies. *J Virol* **69**,
574 1339-1343 (1995).
575
576 36. Menon, M., Hussell, T. & Ali Shuwa, H. Regulatory B cells in respiratory health and
577 diseases. *Immunol Rev* **299**, 61-73 (2021).
578
579 37. Rosato, P.C., Beura, L.K. & Masopust, D. Tissue resident memory T cells and viral
580 immunity. *Curr Opin Virol* **22**, 44-50 (2017).
581
582 38. Son, Y.M. *et al.* Tissue-resident CD4(+) T helper cells assist the development of
583 protective respiratory B and CD8(+) T cell memory responses. *Sci Immunol* **6** (2021).
584
585 39. Pruner, K.B. & Pepper, M. Local memory CD4 T cell niches in respiratory viral
586 infection. *J Exp Med* **218** (2021).
587
588 40. Swadling, L. *et al.* Pre-existing polymerase-specific T cells expand in abortive
589 seronegative SARS-CoV-2. *Nature* **601**, 110-117 (2022).
590
591 41. Ewer, K.J. *et al.* T cell and antibody responses induced by a single dose of ChAdOx1
592 nCoV-19 (AZD1222) vaccine in a phase 1/2 clinical trial. *Nature Medicine* **27**, 270-278
593 (2021).
594
595 42. Moss, P. The T cell immune response against SARS-CoV-2. *Nature Immunology* **23**,
596 186-193 (2022).
597
598 43. Sahin, U. *et al.* BNT162b2 vaccine induces neutralizing antibodies and poly-specific T
599 cells in humans. *Nature* **595**, 572-577 (2021).
600
601 44. Heinz, F.X. & Stiasny, K. Distinguishing features of current COVID-19 vaccines:
602 knowns and unknowns of antigen presentation and modes of action. *npj Vaccines* **6**,
603 104 (2021).
604
605 45. Lewis, D. Mix-and-match COVID vaccines: the case is growing, but questions remain.
606 *Nature* **595**, 344-345 (2021).
607
608 46. Grifoni, A. *et al.* Targets of T Cell Responses to SARS-CoV-2 Coronavirus in Humans
609 with COVID-19 Disease and Unexposed Individuals. *Cell* (2020).
610
611 47. Pang, N.Y.-L., Pang, A.S.-R., Chow, V.T. & Wang, D.-Y. Understanding neutralising
612 antibodies against SARS-CoV-2 and their implications in clinical practice. *Military*
613 *Medical Research* **8**, 47 (2021).
614
615 48. Mitsi, E. *et al.* PCV13 induced IgG responses in serum associate with serotype-
616 specific IgG in the lung. *J Infect Dis* (2021).
617

bioRxiv preprint doi: https://doi.org/10.1101/2023.01.25.525485; this version posted January 25, 2023. The copyright holder for this preprint (which was not certified by peer review) is the author/funder, who has granted bioRxiv a license to display the preprint in perpetuity. It is made available under aCC-BY-ND 4.0 International license.

618 49. Carniel, B.F. *et al.* Pneumococcal colonization impairs mucosal immune responses to
619 live attenuated influenza vaccine. *JCI Insight* **6** (2021).
620
621 50. Dagan, R. *et al.* Modeling pneumococcal nasopharyngeal acquisition as a function of
622 anticapsular serum antibody concentrations after pneumococcal conjugate vaccine
623 administration. *Vaccine* **34**, 4313-4320 (2016).
624
625 51. Maringer, Y. *et al.* Durable spike-specific T-cell responses after different COVID-19
626 vaccination regimens are not further enhanced by booster vaccination. *Sci Immunol*,
627 eadd3899 (2022).
628
629 52. Reynolds, C.J. *et al.* Prior SARS-CoV-2 infection rescues B and T cell responses to
630 variants after first vaccine dose. *Science* **372**, 1418-1423 (2021).
631
632 53. Crotty, S. Hybrid immunity. *Science* **372**, 1392-1393 (2021).
633
634 54. Teijaro, J.R. *et al.* Cutting edge: Tissue-retentive lung memory CD4 T cells mediate
635 optimal protection to respiratory virus infection. *J Immunol* **187**, 5510-5514 (2011).
636
637 55. Wilkinson, T.M. *et al.* Preexisting influenza-specific CD4+ T cells correlate with
638 disease protection against influenza challenge in humans. *Nat Med* **18**, 274-280
639 (2012).
640
641 56. Hassan, A.O. *et al.* A Single-Dose Intranasal ChAd Vaccine Protects Upper and Lower
642 Respiratory Tracts against SARS-CoV-2. *Cell* **183**, 169-184 e113 (2020).
643
644 57. Hassan, A.O. *et al.* A single intranasal dose of chimpanzee adenovirus-vectored
645 vaccine protects against SARS-CoV-2 infection in rhesus macaques. *Cell Rep Med* **2**,
646 100230 (2021).
647
648 58. Mao, T. *et al.* Unadjuvanted intranasal spike vaccine elicits protective mucosal
649 immunity against sarbecoviruses. *Science*, eabo2523 (2022).
650
651 59. Lapuente, D. *et al.* Protective mucosal immunity against SARS-CoV-2 after
652 heterologous systemic prime-mucosal boost immunization. *Nat Commun* **12**, 6871
653 (2021).
654
655 60. Madhavan, M. *et al.* Tolerability and immunogenicity of an intranasally-administered
656 adenovirus-vectored COVID-19 vaccine: An open-label partially-randomised
657 ascending dose phase I trial. *eBioMedicine* **85** (2022).
658
659 61. Zaidi, S.R. *et al.* Single use and conventional bronchoscopes for Broncho alveolar
660 lavage (BAL) in research: a comparative study (NCT 02515591). *BMC Pulmonary*
661 *Medicine* **17**, 83 (2017).
662

bioRxiv preprint doi: https://doi.org/10.1101/2023.01.25.525485; this version posted January 25, 2023. The copyright holder for this preprint (which was not certified by peer review) is the author/funder, who has granted bioRxiv a license to display the preprint in perpetuity. It is made available under aCC-BY-ND 4.0 International license.

663 62. Mitsi, E. *et al.* Nasal Pneumococcal Density Is Associated with Microaspiration and
664 Heightened Human Alveolar Macrophage Responsiveness to Bacterial Pathogens.
665 *Am J Respir Crit Care Med* **201**, 335-347 (2020).
666
667 63. Mitsi, E. *et al.* Streptococcus pneumoniae colonization associates with impaired
668 adaptive immune responses against SARS-CoV-2. *J Clin Invest* (2022).
669
670 64. Dan, J.M. *et al.* Immunological memory to SARS-CoV-2 assessed for up to 8 months
671 after infection. *Science* **371** (2021).
672
673 65. Le Bert, N. *et al.* SARS-CoV-2-specific T cell immunity in cases of COVID-19 and SARS,
674 and uninfected controls. *Nature* **584**, 457-462 (2020).
675

Table 1: Characteristics of participants

Characteristics	**Controls (n=11)**	**Vaccinated (n=7)**	**Infected &Vaccinated (n=15)**
Age (yr), median (IQR)	21 (19 – 24)	25 (23 – 41)	43 (20 – 52)
Female, n (%)	7 (64%)	4 (57%)	10 (67%)
Time since symptomatic infection in days, median (min – max)	n/a	n/a	273 (201 – 570)
NIH clinical score, median (IQR)	n/a	n/a	4 (3-4)
Vaccination history			
Vaccine type	n/a	BNT162b2, n=5 ChAdOx1_S, n=2	BNT162b2, n=9 Moderna, n=1 ChAdOx1_S, n=5
Time since 2nd vaccine dose in days, median (min – max)	n/a	113 (23 – 186)	73 (23 -160)

bioRxiv preprint doi: https://doi.org/10.1101/2023.01.25.525485; this version posted January 25, 2023. The copyright holder for this preprint (which was not certified by peer review) is the author/funder, who has granted bioRxiv a license to display the preprint in perpetuity. It is made available under aCC-BY-ND 4.0 International license.

Figure 1. Systemic and lung mucosa antibody responses following vaccination alone and hybrid immunity. A) Schematic of study groups depicting SARS-CoV-2 vaccination status, sample collection per group and immunological parameters analysed. Pre-pandemic controls (n=11), infection-naïve vaccinated individual (naïve vaccinated group, n=7) and vaccinated individuals with exposure to SARS-CoV-2 (infected vaccinated or hybrid immunity group, n=15). Different colours used to depict convalescents with asymptomatic or symptomatic SARS-CoV-2 infection. **(B to E)** Levels of IgG against Spike (B and D) and RBD (C and E) in serum and bronchoalveolar lavage (BAL) fluid of control (n=11), vaccinated (n=7) and infected vaccinated donors (n=15). **(F to G)** Levels of IgA against Spike (F) and RDB (G) in BAL fluid of control (n=11), vaccinated (n=7) and infected, vaccinated donors (n=15). Antibody levels are expressed as arbitrary units. Homologous vaccination with ChAdOX1_S or mRNA vaccine is depicted with an open or close circle, respectively. Data shown are in median and interquartile range (IQR). Statistical differences were determined by Kruskal-Wallis test following correction for multiple comparisons. Adjusted p values are indicated by *($p < 0.05$), **($p < 0.01$) and ****($p < 0.0001$).

Extended Data Figure 1. Associations between lung mucosa and systemic antibody levels against Spike post SARS-CoV-2 vaccination. (A to C) Levels of anti-N IgG in serum (A) and anti-N IgG (B) and IgA (C) in BAL fluid of control (n=11), naïve vaccinated (n=7) and infected vaccinated donors (n=15). Correlation of anti-S IgG **(D)** and anti-S IgA **(E)** levels measured in serum and BAL fluid of naïve, vaccinated (in turquoise) and infected, vaccinated donors (in purple). Total n=22 vaccinated individuals. R and p values are shown using Spearman rank correlation.

Figure 2. Detectable anti-SARS-CoV-2 memory B cell responses in the lung mucosa following infection and vaccination. A) Example flow cytometry plots of Spike-, RBD- and N-specific global memory B cells (MBCs) in PBMC and BAL sample of an unexposed pre-pandemic control (left) and an infected vaccinated donor(right) (see extended data fig.2 for full gating). **B-D)** Frequency of circulating Spike-, RBD- and N-specific MBCs in control (n=10), naïve, vaccinated (n=7) and infected, vaccinated donors (n=15). **E-G)** Frequency of Spike-, RBD- and N-specific MBCs detected in BAL samples of control (n=6) and infected vaccinated donors (n=9). **H)** Frequency of SARS-CoV-2 specific memory B cells in blood (PBMC) and BAL, shown as paired samples, of infected vaccinated donors. **(I)** Distribution of global MBC subsets in PBMC and BAL based on the expression of IgD and IgM in control and infected, vaccinated donors together (n=25). Homologous vaccination with ChAdOX1_S or mRNA

bioRxiv preprint doi: https://doi.org/10.1101/2023.01.25.525485; this version posted January 25, 2023. The copyright holder for this preprint (which was not certified by peer review) is the author/funder, who has granted bioRxiv a license to display the preprint in perpetuity. It is made available under aCC-BY-ND 4.0 International license.

vaccine is depicted with an open or close circle, respectively. Data shown are in median and interquartile range (IQR). Statistical differences were determined by Kruskal-Wallis test following correction for multiple comparisons **(B-D)**, Mann-Whitney U test **(E-G)** and Wilcoxon's paired test **(H-I).** P values are indicated by *(p < 0.05), **(p < 0.01), ***(p < 0.001) and ****(p < 0.0001).

Extended Data Figure 2. Memory B cells and SARS-CoV-2 specific B cells responses in human blood and BAL. **A)** Gating strategy of B cells in human PBMC or BAL sample, with representative flow cytometry plots of SARS-CoV-2 specific B cells from controls and infected, vaccinated donors. **B)** Frequency of circulating SARS-CoV-2 MBCs in mRNA (n=10) or ChAdOxAd1_S vaccine (n=5) recipients with prior infection. **C)** Frequency of lower airway Spike MBCs in mRNA (close circles, n=6) or ChAdOxAd1_S vaccine (open circles, n=3) recipients with prior infection. Data shown are in median and interquartile range (IQR). Statistical differences were determined by Mann-Whitney U test**.** P values are indicated by *(p < 0.05), **(p < 0.01) and ****(p < 0.0001).

Figure 3. Detection of S-specific T cells responses in the lung mucosa after infection and vaccination but not following vaccination alone. A) Representative flow cytometry plots of S-specific $CD4^+$ and $CD8^+$ T cells in PBMC and BAL sample (on the left) and S-specific TRM $CD4^+$ and $CD8^+$ T cells in BAL sample (on the right) of an infected, vaccinated donor. Identification of Spike specific T cells was based on the AIM assay, assessing co-expression CD40L and OX40 on $CD4^+$ T cells and co-expression of CD25 and 4-1BB on $CD8^+$ T cells after stimulation with Spike megapools. **B-C)** Frequency of circulating S-specific $CD4^+$ and $CD8^+$ T cells in control (n=8), naïve, vaccinated (n= 6) and infected, vaccinated donors (n= 13). **D-G)** Frequency of lower-airway S-specific $CD4^+$ and $CD8^+$ T cells within the global (D-E) and TRM compartment (F-G) in control (n=8), naïve, vaccinated (n= 6) and infected, vaccinated donors (n= 13). **H-I)** Frequency of S-specific $CD4^+$ and $CD8^+$ T cells in PBMC and BAL, shown as paired samples, of naïve, vaccinated, and infected vaccinated donors. Homologous vaccination with ChAdOX1_S or mRNA vaccine is depicted with an open or close circle, respectively. Data shown are in median and interquartile range (IQR). Statistical differences were determined by Kruskal-Wallis test following correction for multiple comparisons **(B-G)** and Wilcoxon's paired test **(H-I).** P values are indicated by *(p < 0.05), **(p < 0.01), ***(p < 0.001) and ****(p < 0.0001).

Extended Data Figure 3. A) Example gating of T cell staining after overnight stimulation with SARS-CoV-2 peptide pools. Lymphocytes (SSC-H vs. FSC-H), single cells (FSC-H vs. FSC-

bioRxiv preprint doi: https://doi.org/10.1101/2023.01.25.525485; this version posted January 25, 2023. The copyright holder for this preprint (which was not certified by peer review) is the author/funder, who has granted bioRxiv a license to display the preprint in perpetuity. It is made available under aCC-BY-ND 4.0 International license.

A), Live cells (fixable live/dead), $CD3^+$, $CD4^+$ or $CD8^+$ or MAIT cells. Tissue resident memory (TRM) $CD4^+$ and $CD8^+$ T cells were defined as $CD4^+CD69^+CD49a^+$ and $CD8^+CD69^+CD103^+$, respectively. **B)** Representative plots of SARS-CoV-2 specific $CD4^+$ and $CD8^+$ T cells in PBMC and BAL of an infected, vaccinated donor after overnight stimulation with SARS-CoV-2 peptide pools. DMSO was used as a negative control. **B-C)** Frequency of circulating and lower-airway S-specific $CD4^+$ and $CD8^+$ T cells in mRNA (n=9) or ChAdOxAd1_S vaccine (n=5) recipients with prior infection. **D-E)** Paired analysis of proportions of $CD4^+$ and $CD8^+$ T cells which recognise SARS-CoV-2 antigens in BAL and paired blood. Statistical differences were determined by Mann-Whitney U test**.** *($p < 0.05$).

Figure 4. Detection of infection-induced SARS-CoV-2 T cell responses in the periphery and lung mucosa. A-B) Frequency of circulating N-, M- and RTC-specific $CD4^+$ and $CD8^+$ T cells in control (n=8), naïve, vaccinated (n= 6) and infected, vaccinated donors (n= 13). **C-F)** Frequency of N-, M- and RTC-specific $CD4^+$ and $CD8^+$ T cells within the global and TRM compartment of lower airway T cells in control (n=4) and infected, vaccinated donors (n=8). **G-H)** Frequency of SARS-CoV-2-specific $CD4^+$ and $CD8^+$ T cells in PBMC and BAL, shown as paired samples, of infected, vaccinated donors. Homologous vaccination with ChAdOX1_S or mRNA vaccine is depicted with an open or close circle, respectively. Data shown are in median and interquartile range (IQR). Statistical differences were determined by Kruskal-Wallis test following correction for multiple comparisons **(A-B)**, Mann-Whitney U test **(E-F)** and Wilcoxon's paired test **(G-H).** P values are indicated by *($p < 0.05$) and **($p < 0.01$).

Figure 5. Long-lived IgG but short-term IgA responses to SARS-CoV-2 antigens in the lung mucosa following vaccination and infection. A-B) Correlation between time post-vaccination and levels of IgG to S, RBD and N proteins measured in serum (A) and BAL supernatant (B) of naïve vaccinated (n=7) and infected vaccinated individuals (n=15). **C)** Correlation between time post-vaccination and levels of IgA to S, RBD and N proteins measured in BAL supernatant of of naïve, vaccinated (n=7) and infected, vaccinated individuals (n=15). Homologous vaccination with ChAdOX1_S or mRNA vaccine is depicted with an open or close circle, respectively. Spearman correlation used. R and p values are shown.

Figure 6. Persistent S-specific T cells in the lung mucosa following hybrid immunity. A) Correlation between time post-vaccination and the frequency of S-specific $CD4^+$ (left) and $CD8^+$ T cells (right) detected in the blood of naïve vaccinated (n=6) and infected vaccinated individuals (n=15). **B-C)** Correlation between time post-vaccination and the frequency of S-specific $CD4^+$ (left) and $CD8^+$ T cells (right) in the global and TRM compartment of lower-

bioRxiv preprint doi: https://doi.org/10.1101/2023.01.25.525485; this version posted January 25, 2023. The copyright holder for this preprint (which was not certified by peer review) is the author/funder, who has granted bioRxiv a license to display the preprint in perpetuity. It is made available under aCC-BY-ND 4.0 International license.

airway T cells in BAL of naïve, vaccinated (n=6) and infected, vaccinated individuals (n=15). Homologous vaccination with ChAdOX1_S or mRNA vaccine is depicted with an open or close circle, respectively. D) Correlation between time post infection from symptoms onset and the frequency of N-, M and RTC- specific $CD4^+$ (left) and $CD8^+$ T cells (right) detected in BAL of infected, vaccinated individuals with symptomatic, PCR-confirmed SARS-CoV-2 infection (n=13). Spearman correlation used. R and p values are shown.

bioRxiv preprint doi: https://doi.org/10.1101/2023.01.25.525485; this version posted January 25, 2023. The copyright holder for this preprint (which was not certified by peer review) is the author/funder, who has granted bioRxiv a license to display the preprint in perpetuity. It is made available under aCC-BY-ND 4.0 International license.

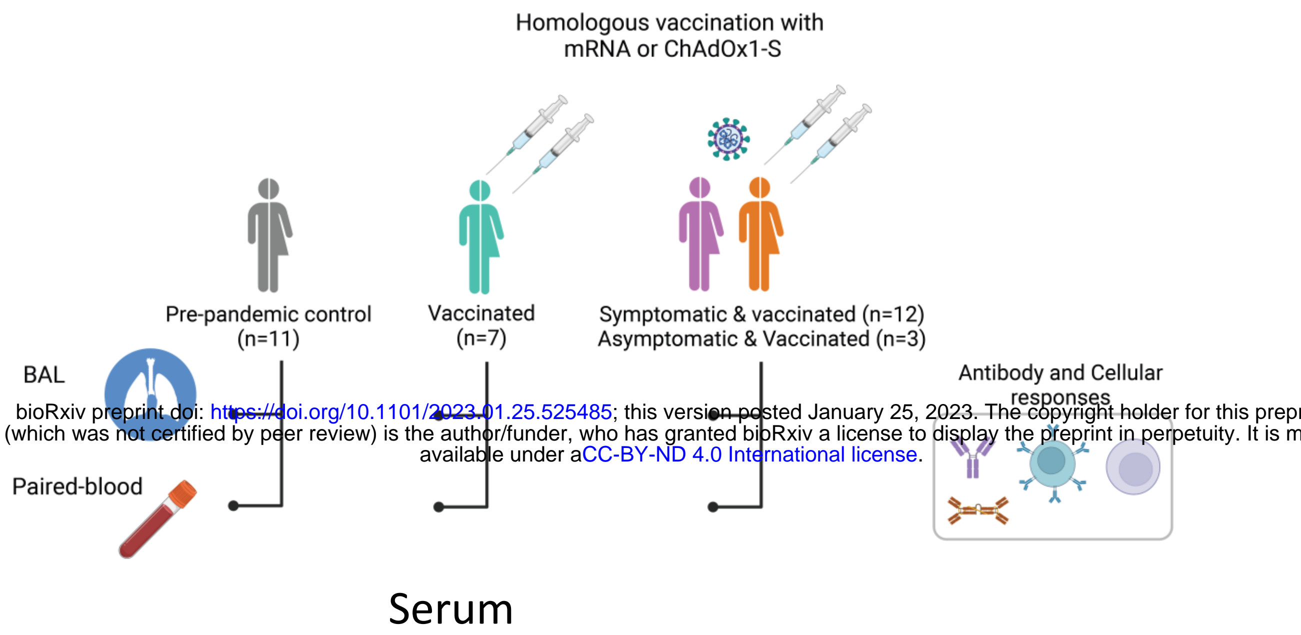

Serum

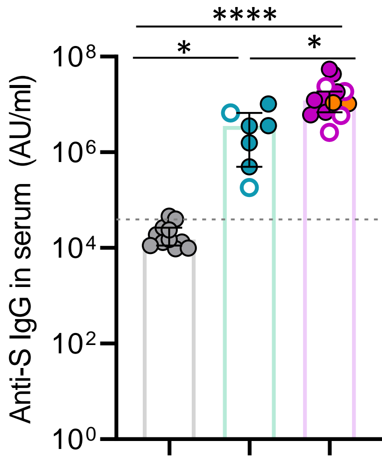

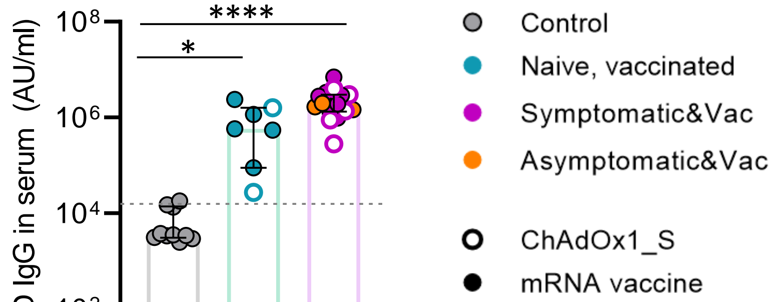

Lung

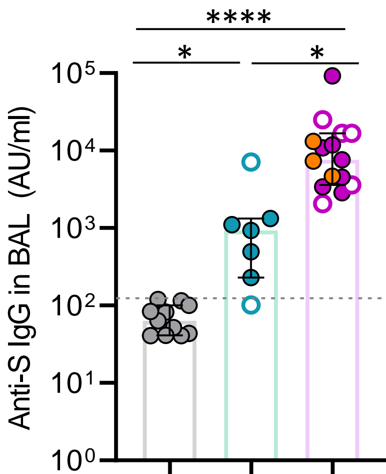

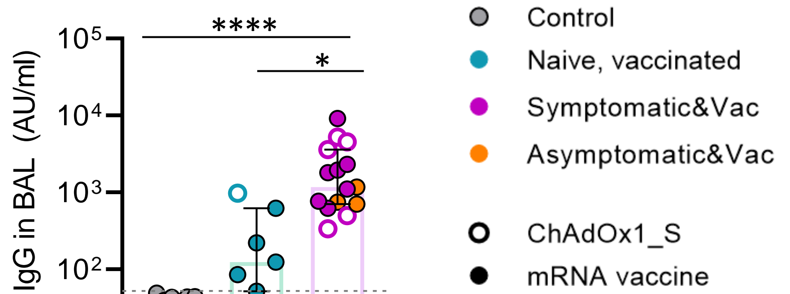

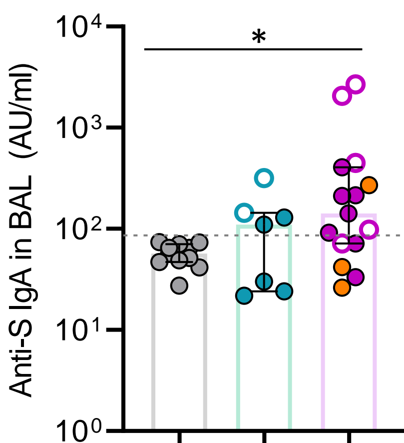

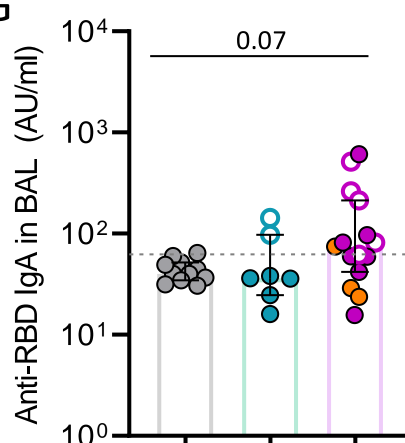

Figure 1

bioRxiv preprint doi: https://doi.org/10.1101/2023.01.25.525485; this version posted January 25, 2023. The copyright holder for this prepr
(which was not certified by peer review) is the author/funder, who has granted bioRxiv a license to display the preprint in perpetuity. It is m
available under aCC-BY-ND 4.0 International license.

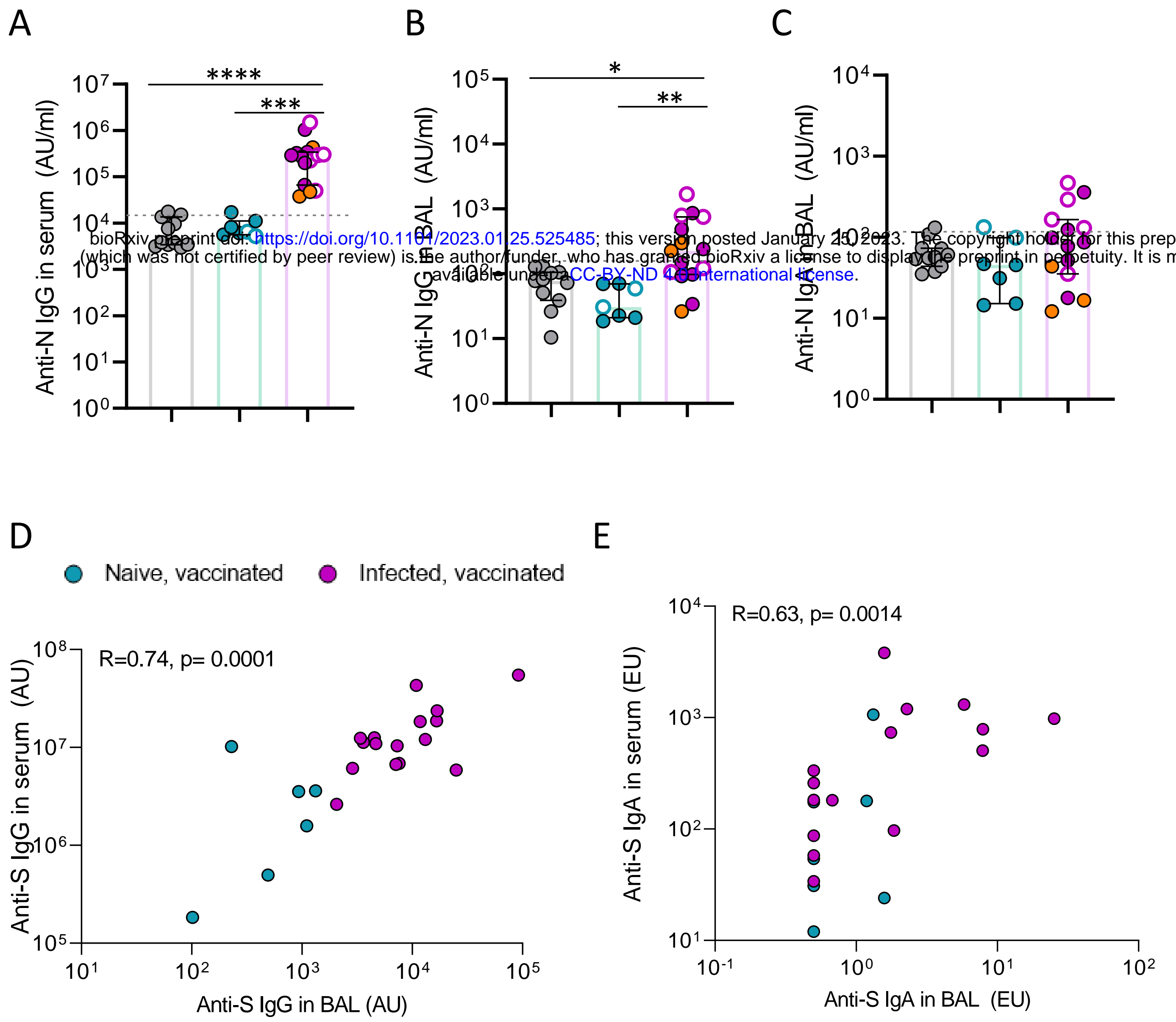

Extended Data Figure 1

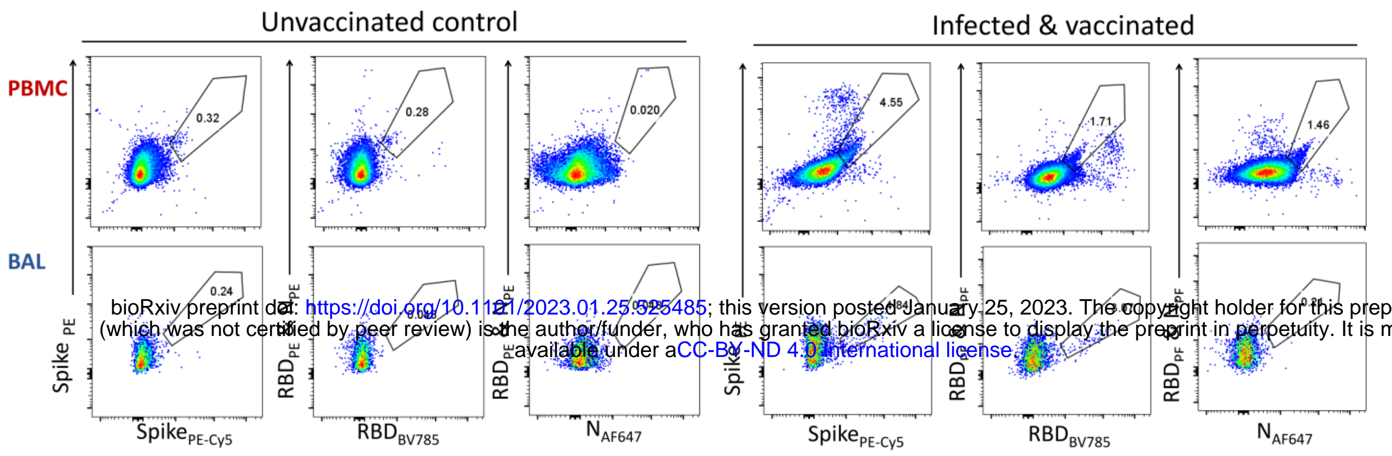

bioRxiv preprint doi: https://doi.org/10.1101/2023.01.25.525485; this version posted January 25, 2023. The copyright holder for this prepr
(which was not certified by peer review) is the author/funder, who has granted bioRxiv a license to display the preprint in perpetuity. It is m
available under aCC-BY-ND 4.0 International license.

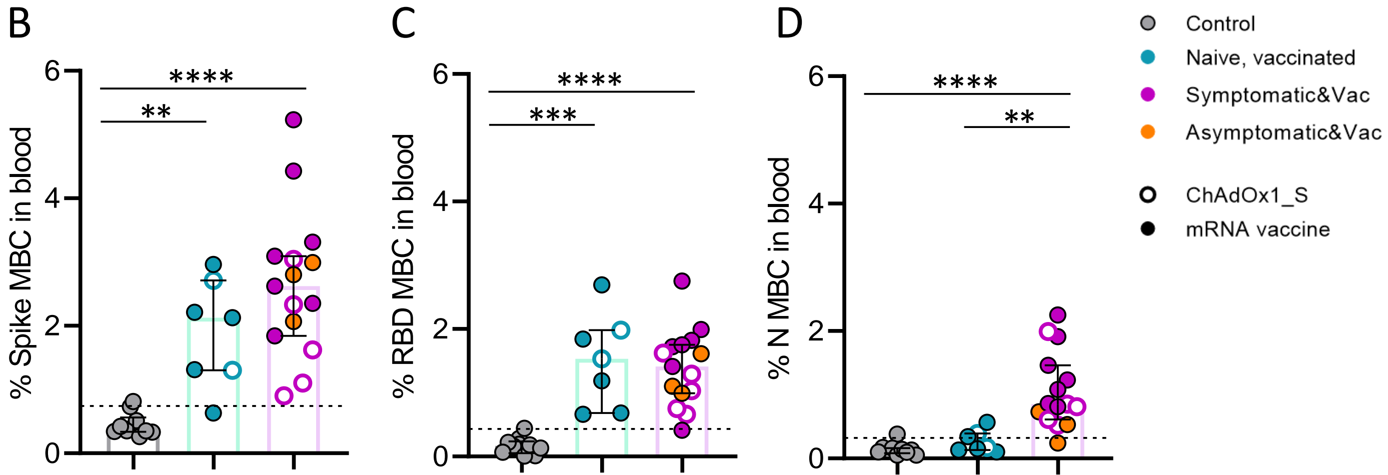

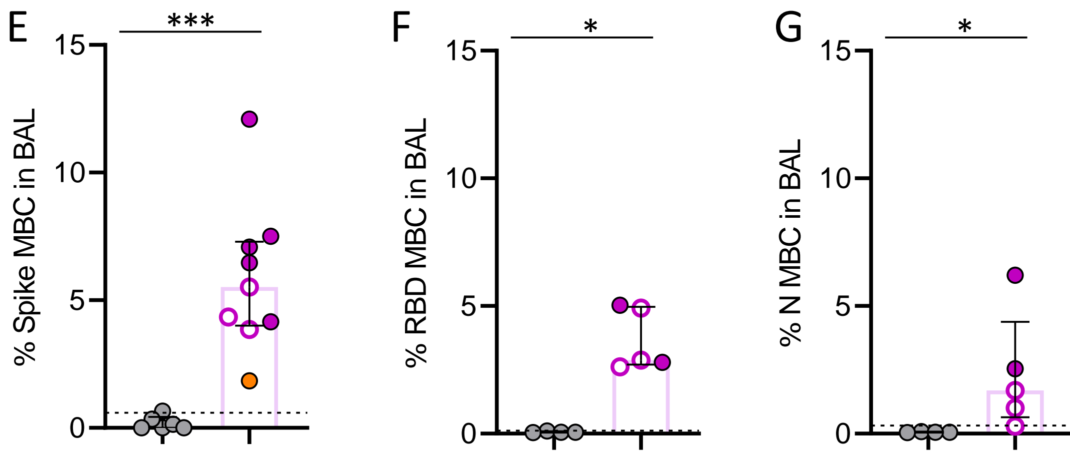

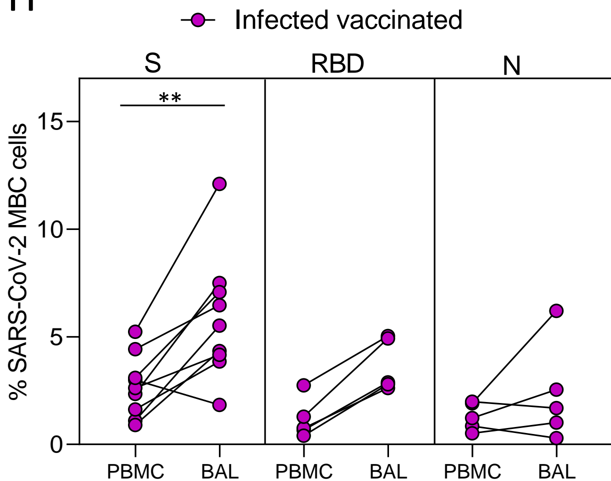

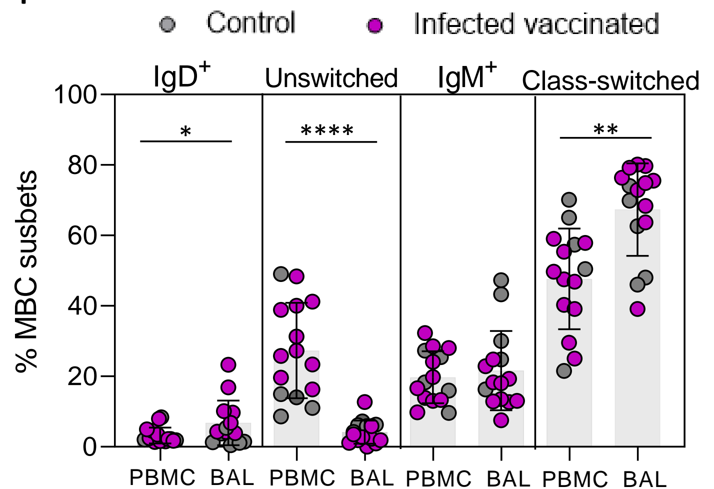

Figure 2

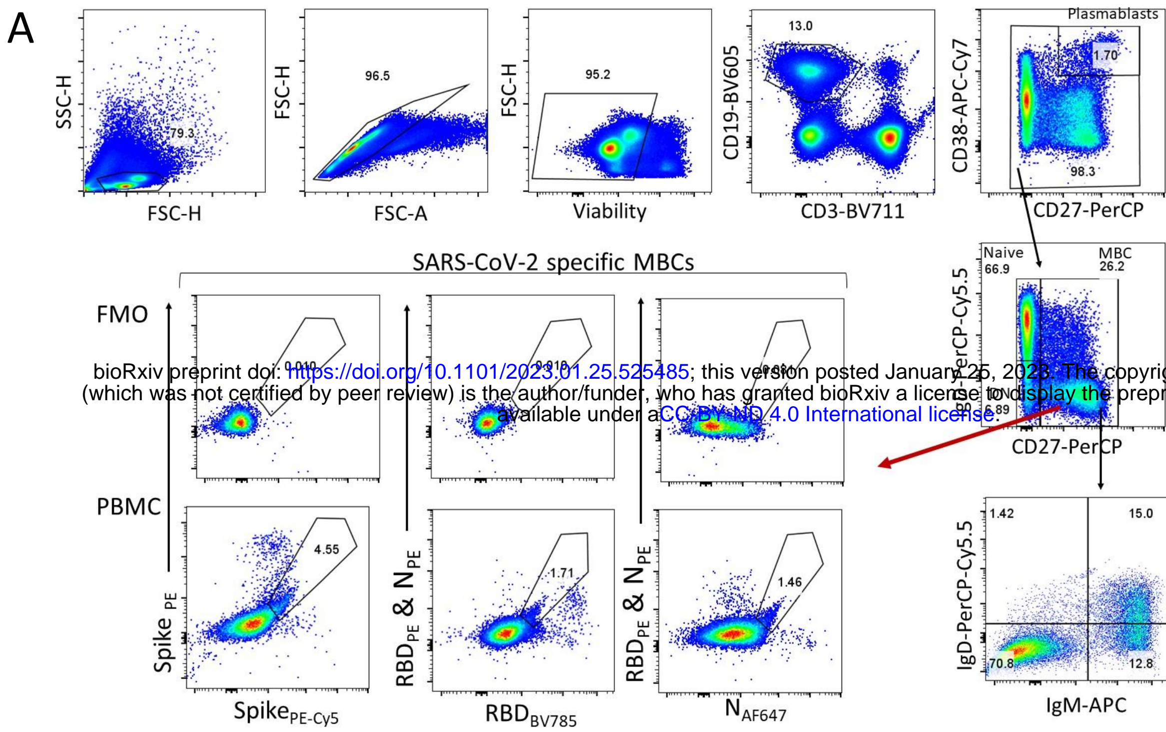

bioRxiv preprint doi: https://doi.org/10.1101/2023.01.25.525485; this version posted January 25, 2023. The copyright holder for this preprint (which was not certified by peer review) is the author/funder, who has granted bioRxiv a license to display the preprint in perpetuity. It is made available under aCC-BY-ND 4.0 International license.

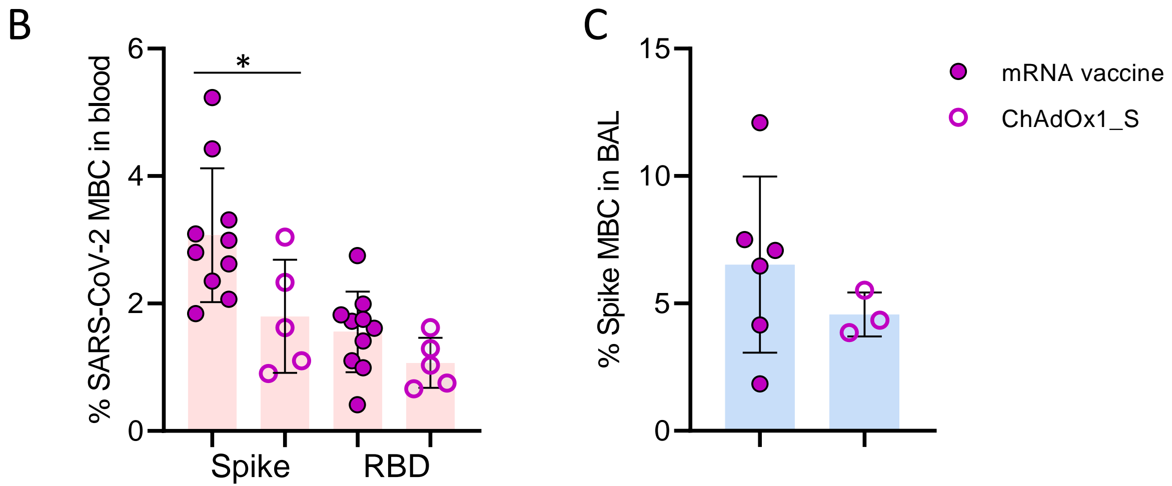

Extended Data Figure 2

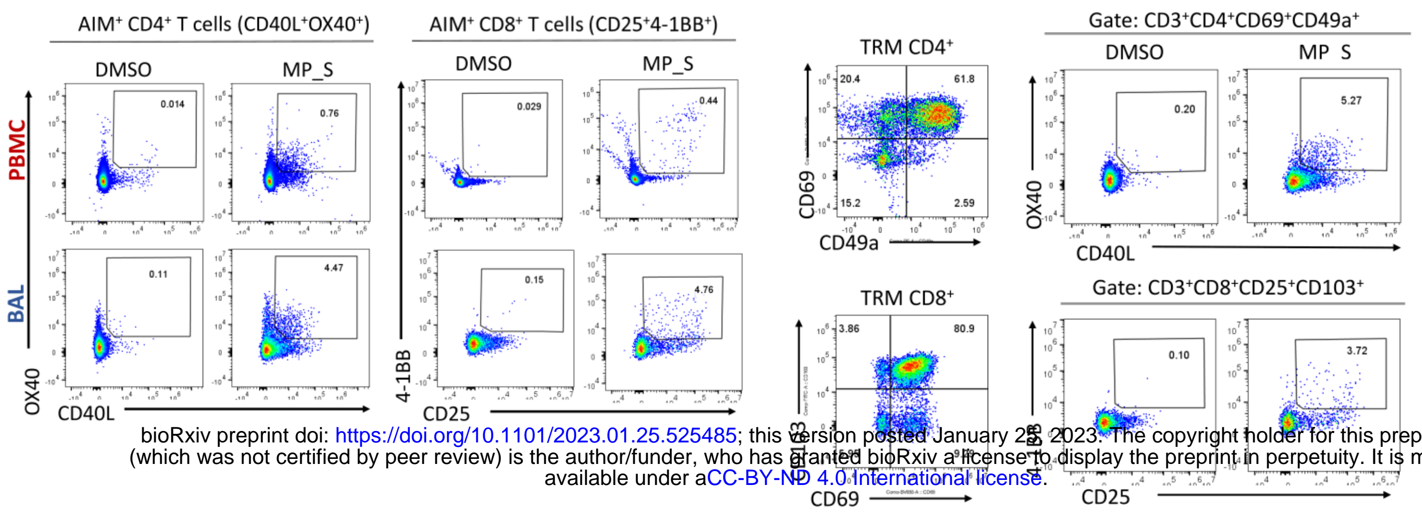

bioRxiv preprint doi: https://doi.org/10.1101/2023.01.25.525485; this version posted January 28, 2023. The copyright holder for this preprint (which was not certified by peer review) is the author/funder, who has granted bioRxiv a license to display the preprint in perpetuity. It is made available under aCC-BY-ND 4.0 International license.

Control
Naive, vaccinated
Symptomatic&Vac
Asymptomatic&Vac
ChAdOx1_S
mRNA vaccine

Blood

BAL

B
% S-specific CD4⁺ T cells
*** *

D
% S-specific CD4⁺ T cells
**** *

F
% S-specific TRM CD4⁺ T cells
*** *

C
% S-specific CD8⁺ T cells
** 0.06

E
% S-specific CD8⁺ T cells
** *

G
% S-specific TRM CD8⁺ T cells
*** *

H
Vaccinated
Infected&Vac
% S-specific CD4⁺ T cells
* ***
PBMC BAL PBMC BAL

I
Vaccinated
Infected&Vac
% S-specific CD8⁺ T cells
ns ***
PBMC BAL PBMC BAL

Figure 3

A

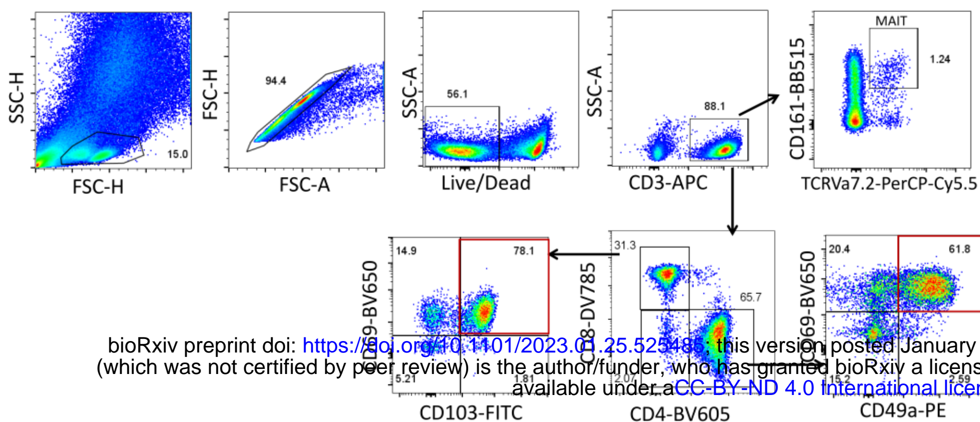

bioRxiv preprint doi: https://doi.org/10.1101/2023.01.25.525485; this version posted January 25, 2023. The copyright holder for this preprint (which was not certified by peer review) is the author/funder, who has granted bioRxiv a license to display the preprint in perpetuity. It is made available under aCC-BY-ND 4.0 International license.

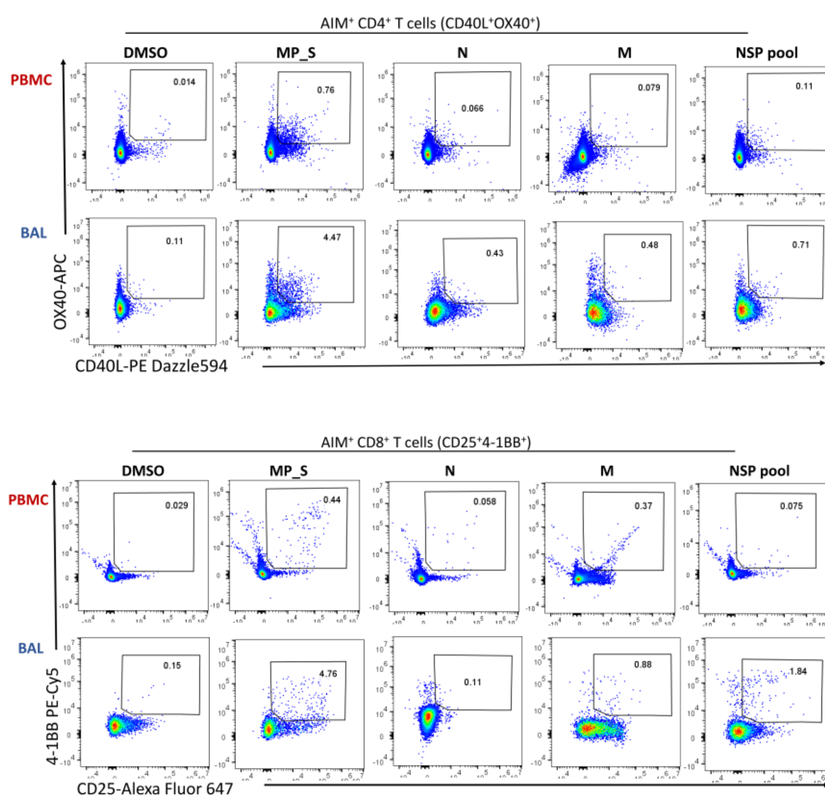

B

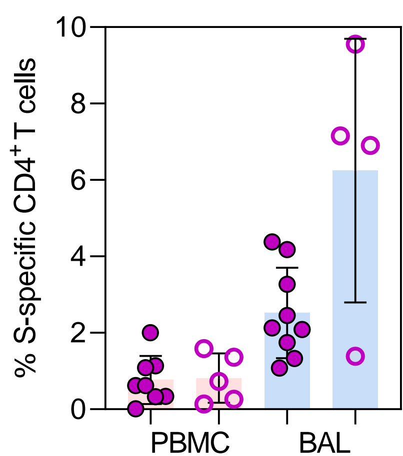

C

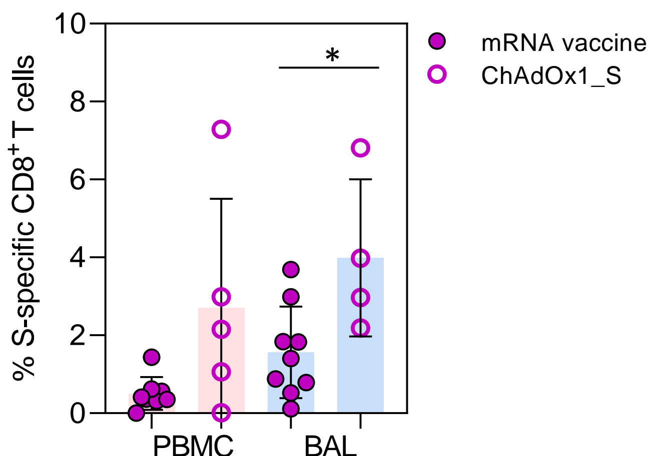

D

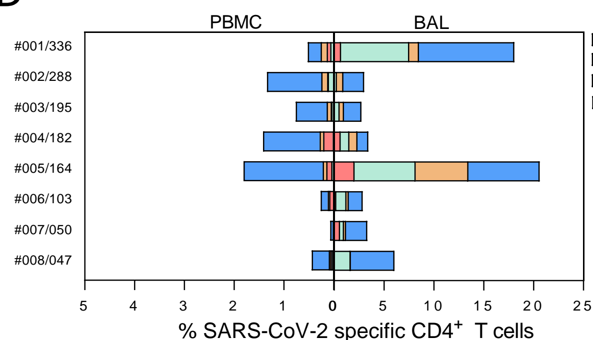

E

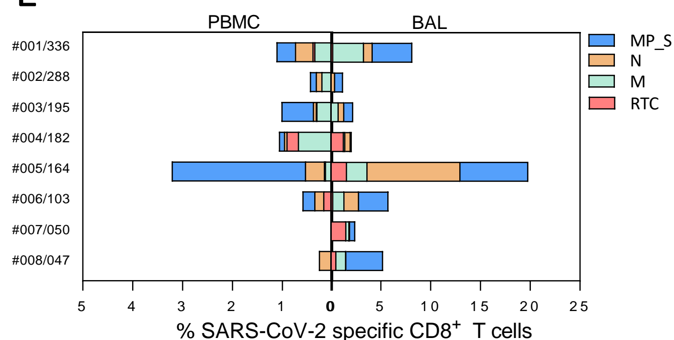

Extended Data Figure 3

Blood

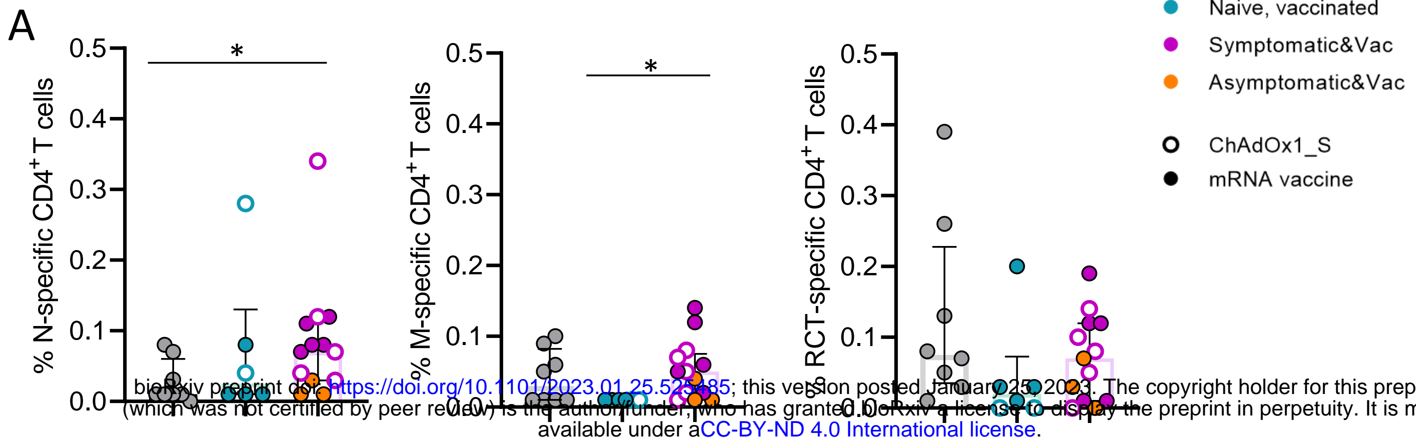

bioRxiv preprint doi: https://doi.org/10.1101/2023.01.25.525485; this version posted January 25, 2023. The copyright holder for this preprint (which was not certified by peer review) is the author/funder, who has granted bioRxiv a license to display the preprint in perpetuity. It is made available under aCC-BY-ND 4.0 International license.

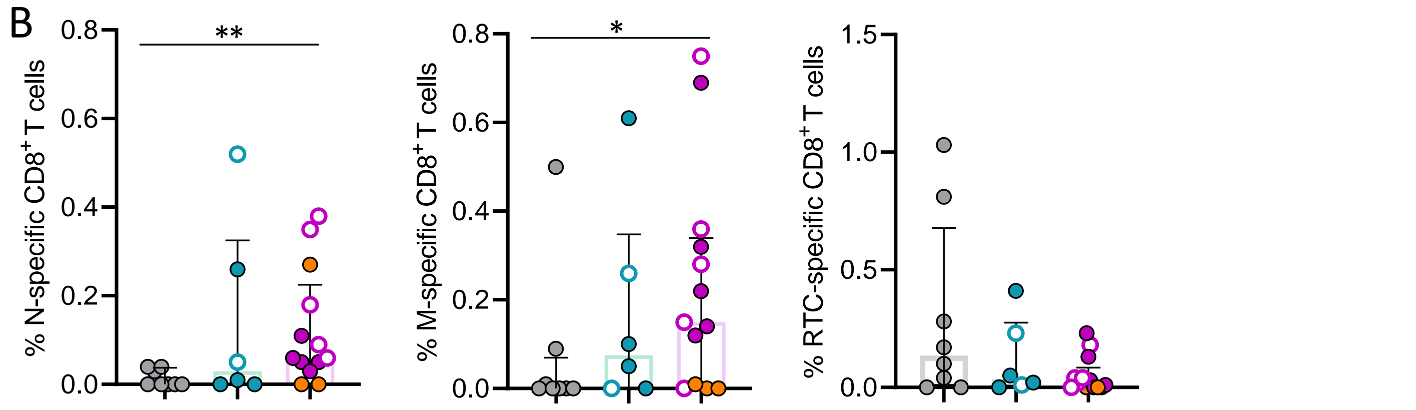

BAL

C

N M RTC

% SARS-CoV-2-specific CD4+ T cells

D

N M RTC

% SARS-CoV-2-specific TRM CD4+ T cells

E

N M RTC

0.05

% SARS-CoV-2-specific CD8+ T cells

F

N M RTC

% SARS-CoV-2-specific TRM CD8+ T cells

G

N M RTC

Infected&Vac

% SARS-CoV-2 CD4+ T cells

PBMC BAL PBMC BAL PBMC BAL

H

N M RTC

Infected&Vac

% SARS-CoV-2 CD8+ T cells

PBMC BAL PBMC BAL PBMC BAL

Figure 4

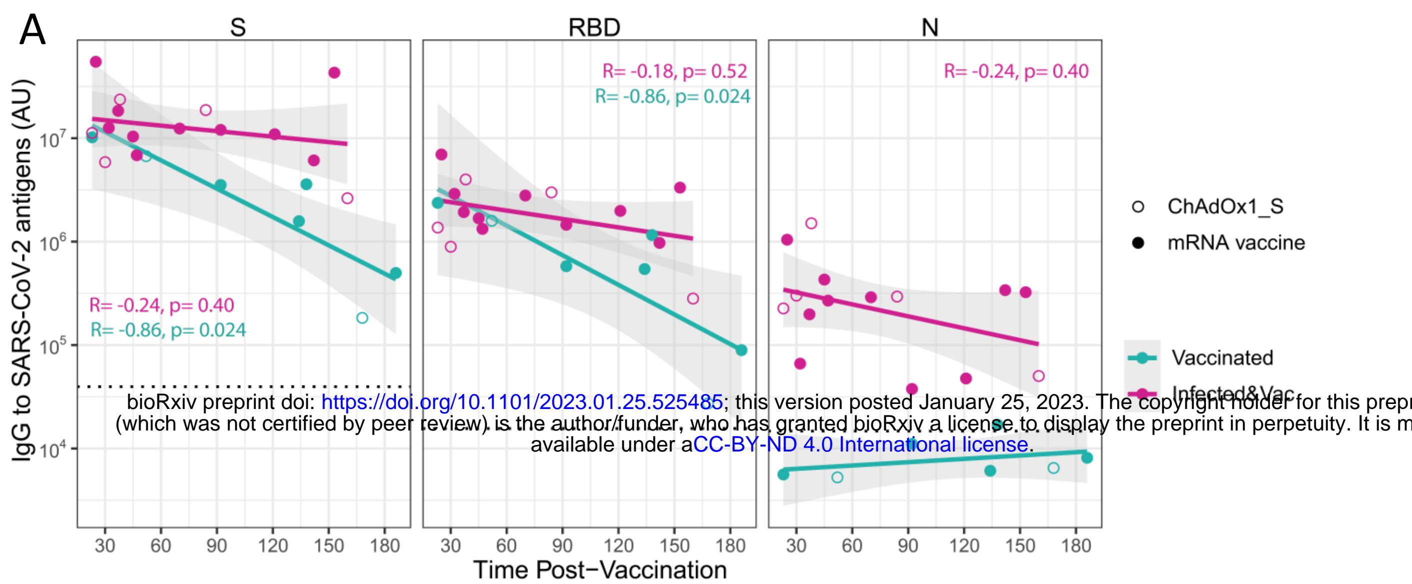

bioRxiv preprint doi: https://doi.org/10.1101/2023.01.25.525485; this version posted January 25, 2023. The copyright holder for this preprint (which was not certified by peer review) is the author/funder, who has granted bioRxiv a license to display the preprint in perpetuity. It is made available under aCC-BY-ND 4.0 International license.

BAL

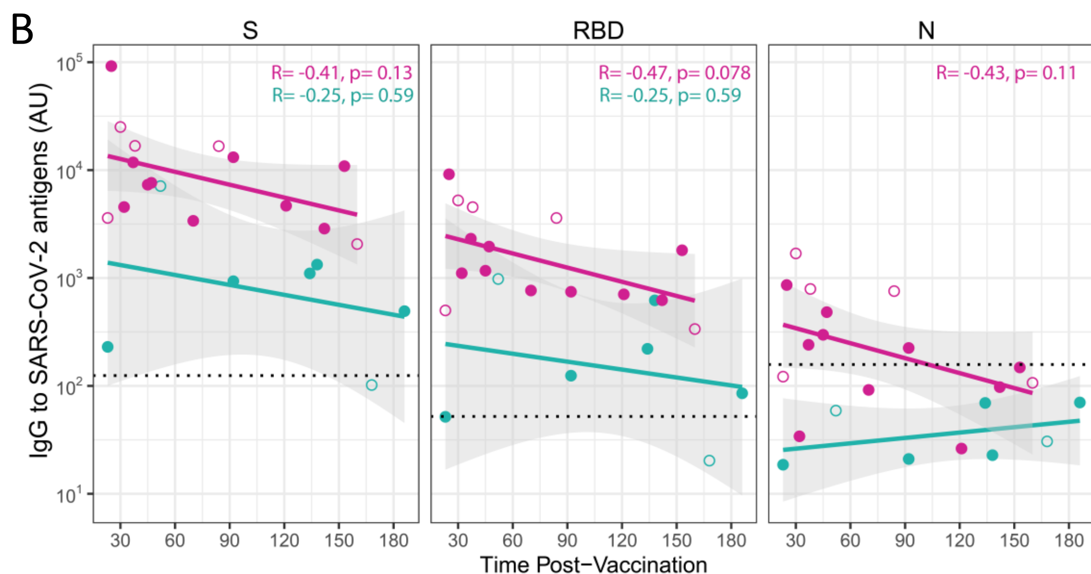

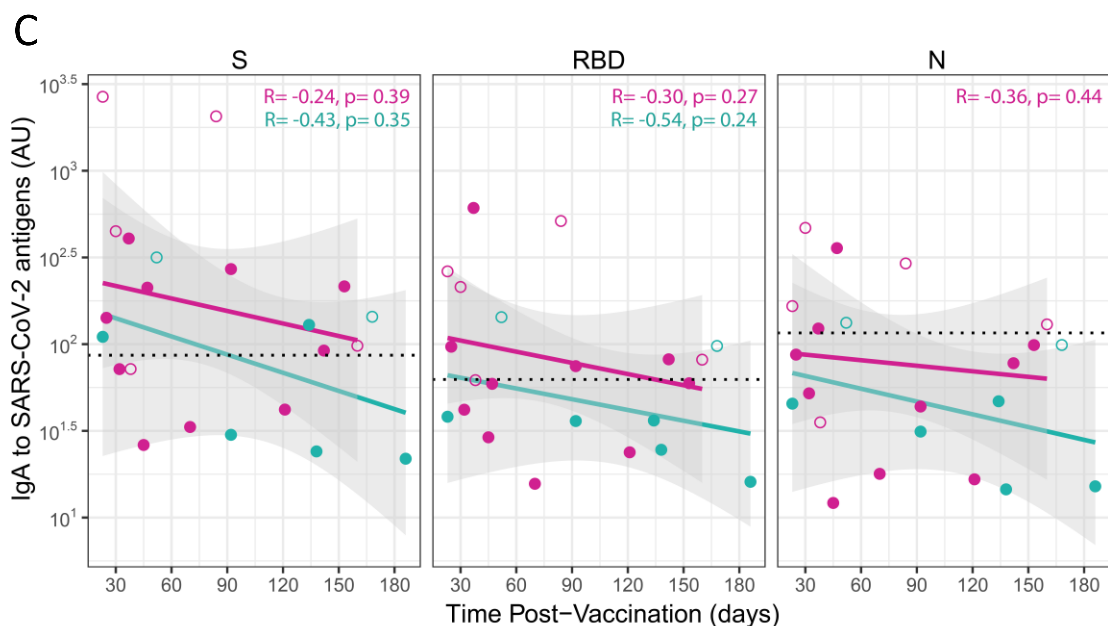

Figure 5

bioRxiv preprint doi: https://doi.org/10.1101/2023.01.25.525485; this version posted January 25, 2023. The copyright holder for this preprint (which was not certified by peer review) is the author/funder, who has granted bioRxiv a license to display the preprint in perpetuity. It is made available under aCC-BY-ND 4.0 International license.

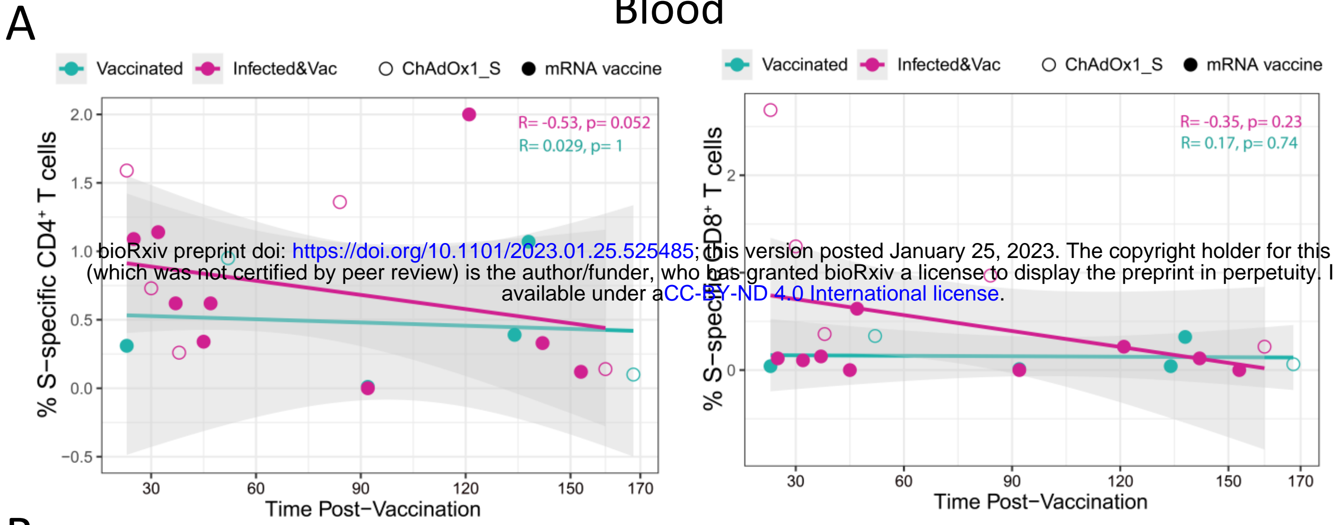

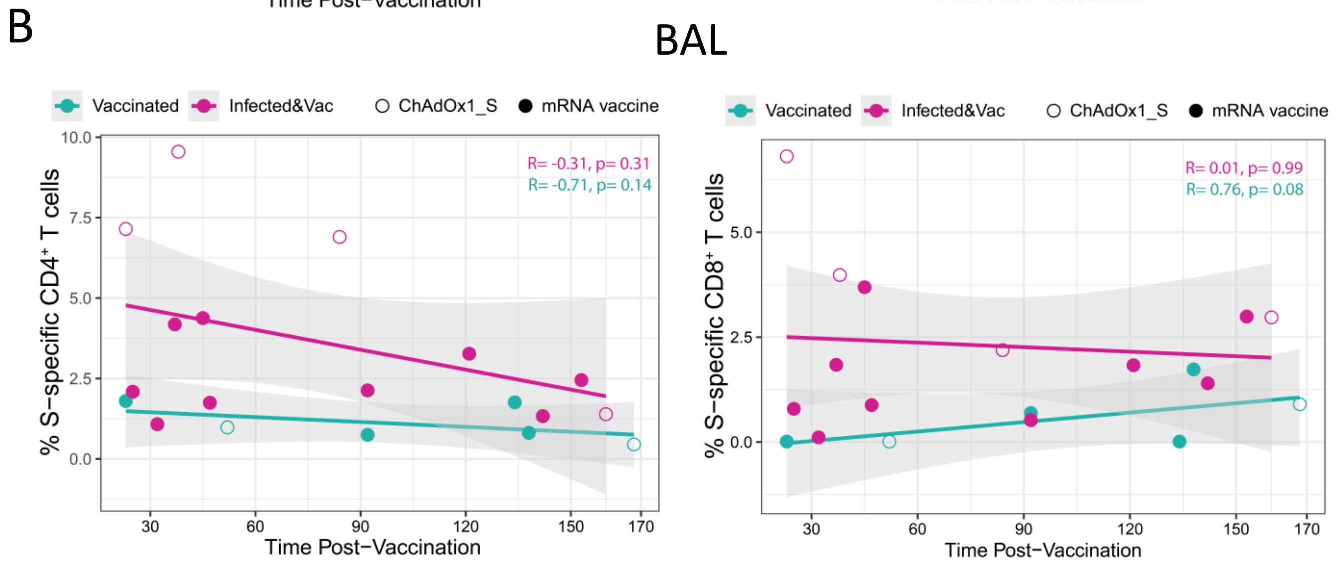

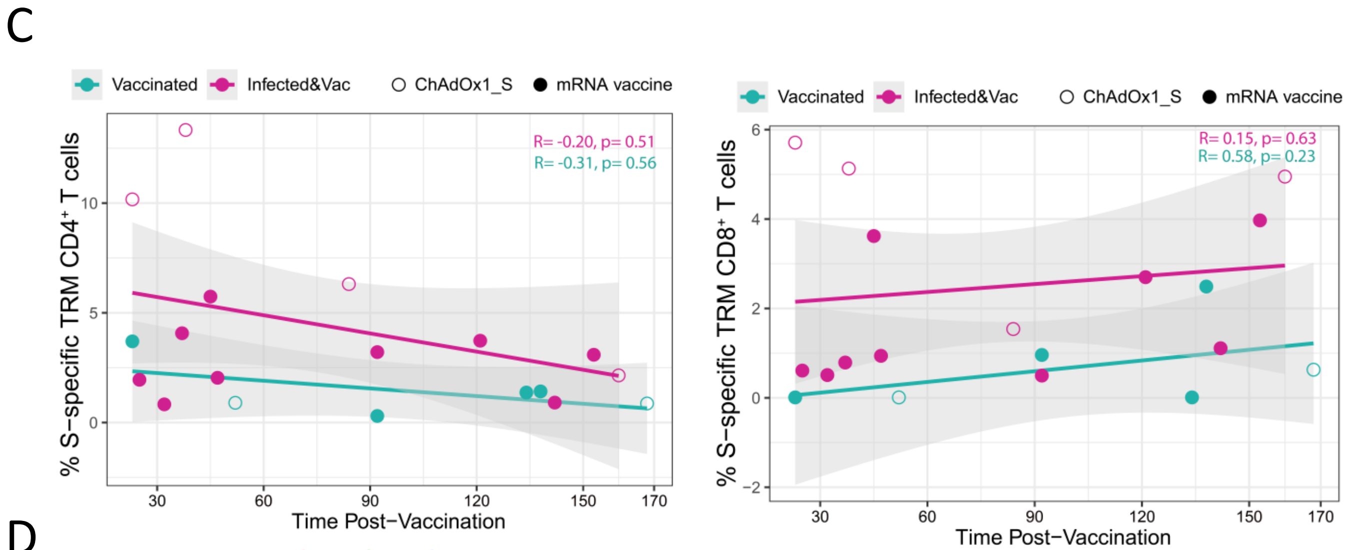

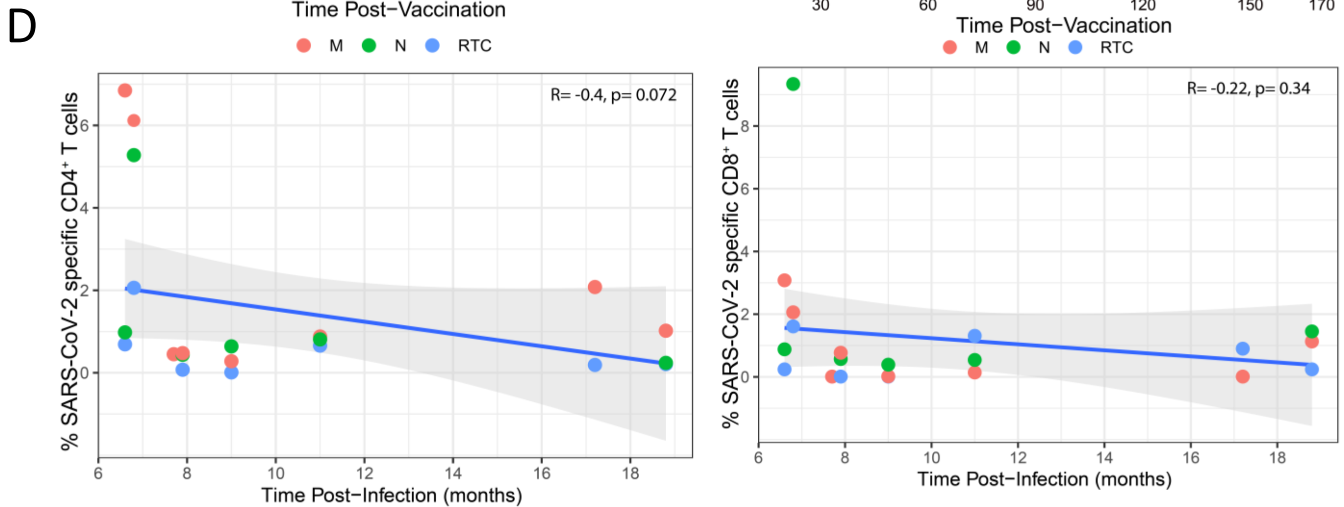

Figure 6